Tight Bounds on 3-Neighbor Bootstrap Percolation

by

Abel Emanuel Romer
B.A.Sc., Quest University Canada, 2017

A Thesis Submitted in Partial Fulfillment of the
Requirements for the Degree of

MASTER OF SCIENCE

in the Department of Mathematics and Statistics

We acknowledge with respect the Lekwungen peoples on whose traditional territory the university stands, and the Songhees, Esquimalt, and W̱SÁNEĆ peoples whose historical relationships with the land continue to this day.

Tight Bounds on 3-Neighbor Bootstrap Percolation

by

Abel Emanuel Romer
B.A.Sc., Quest University Canada, 2017

Supervisory Committee

Dr. Peter Dukes, Co-Supervisor
(Department of Mathematics and Statistics)

Dr. Jonathan Noel, Co-Supervisor
(Department of Mathematics and Statistics)

ABSTRACT

Table of Contents

List of Tables

List of Figures

ACKNOWLEDGEMENTS

DEDICATION

Chapter 1
Introduction

Consider the lattice depicted in the leftmost diagram of Figure 1.1. We refer to the elements of this lattice as *cells*. Suppose we have the capacity to infect some cells (colored red) with a disease, and that this disease will, over a period of time, propagate through uninfected cells of the lattice. Let uninfected cells become infected if they are exposed to at least two infected neighboring cells in the vertical and/or horizontal directions. We say that the initial infection is *lethal* if the entire lattice ultimately becomes infected. Here is the puzzle:

Question. *What is the fewest number of infected cells necessary to spawn a lethal infection?*

Before we present the solution, let us take a moment to examine some properties of infectious sets and attempt to characterize what attributes might correspond to lethality. It should not take too long to observe that if an initial infection is in some way "spread too thin," it will be unable to jump between infected areas, leading to gaps in infection, which we refer to as *immune regions*. The perimeter of the lattice is particularly susceptible to this, as vertices there have fewer neighbors from whom they might be exposed. Heuristically, then, a lethal set must have the ability to effectively span the entire lattice, and must be particularly virulent along the perimeter.

With this criteria in mind, we are able to make some educated guesses regarding the specific structure of sets that are likely to be lethal. In particular, we would like to consider the two starting infections illustrated in Figure 1.2. Notice that while Figure

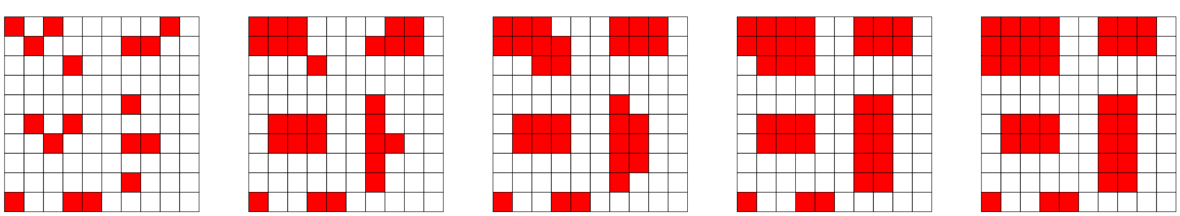

Figure 1.1: An arbitrary set of initially infected cells in the 10×10 lattice, and the stages of infection.

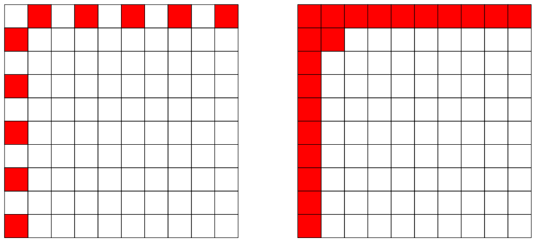

(a) Perimeter construction.

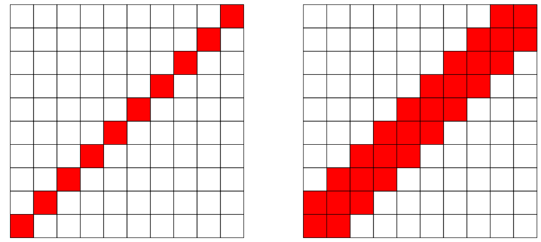

(b) Diagonal construction.

Figure 1.2: Two lethal sets and their resulting infections after one time-step.

1.2 (b) has far fewer perimeter infections, both (a) and (b) manage to form continuous bands of infected cells that appear to span the entire lattice after one step. Indeed, this holds with our notion of immune regions (or lack thereof), and we see that both infections will continue to propagate outwards from these bands until all cells become infected.

It is clear from Figure 1.2 that we may obtain lethal sets on the $n \times n$ lattice of size n by simply infecting the diagonal. What is less obvious is whether it is possible to improve upon this result. Perhaps the most natural first attempt at this is to remove an infection from one of the cells along the diagonal. However, this seems to form an immune region around the removed cell. After some experimentation, one begins to believe it impossible to simultaneously satisfy the heuristic that a starting infection must span the lattice, while also using fewer than n initial infections. The question therefore becomes: how do we prove it?

Consider the cumulative perimeter of infected regions. For a given infectious set A, let $P(A)$ be the total perimeter of the infected regions of A. Let A_0 be an initial infection, and observe that $P(A_0) \leq 4|A_0|$. (This bound is only tight if no two infected cells are adjacent. Otherwise, the edge between such cells lies within the infected region, and cannot contribute to the infection's perimeter.) Observe that for any uninfected cell to become infected, it must abut at least two infected cells. Upon infection, the edges adjacent to these cells no longer lie on the infection's perimeter; additionally, the remaining edges of this newly infected cell contribute at most 2 to this perimeter. All told, after infection, $P(A_1) \leq P(A_0)$.

If we suppose that A_0 is a lethal set, then at some point in time, the entire grid will become infected. This infection will have a perimeter $4n$. Since this perimeter did not increase, A_0 must have originally had a perimeter of at least $4n$. Since each cell in A_0 can contribute at most 4 to this perimeter, it must be the case that $|A_0| \geq n$. Our diagonal construction shows that $|A_0| \leq n$, and so we are able to conclude that n is best possible.

This proof is an instance of the famous *perimeter argument*, which has belonged to bootstrap percolation folklore since at least the work of Pete [**?**]. In the following section, we present generalizations of this argument to higher dimensional rectangular grids.

1.1 Bootstrap Percolation

The study of such cellular infection spread in grids (and more generally in graphs) is known in the literature as *bootstrap percolation*, and was introduced in the 1970s by Chalupa et al. [2] as a simplified model for the behavior of ferromagnetic fields. In their original 1979 paper, the authors research the stable structure of probabilistically selected initial infections. While this differs from the problem posed in Question 1, the rules for the spread of infection and its broad behavior remain the same. It is worth noting that a large portion of contemporary research on bootstrap problems is focused on questions of probabilistic nature; while these problems are certainly interesting and of merit, they do not fall within the scope of this thesis. Rather, we shall focus on those problems where we have specific control over the structure of the initial infections; in particular, we aim to determine the smallest lethal set on the Cartesian product of paths and cycles.

We define the problem in concrete terms. Let G be a graph and $A_0 \subseteq V(G)$ be a set of initially infected vertices. Iteratively, infect those vertices of G with at least r infected neighbors. For all $t > 0$, let A_t be the set of infected vertices at time step t. We then have

$$A_t = A_{t-1} \cup \{v \in V(G) : |N_G(v) \cap A_{t-1}| \geq r\},$$

where $N_G(v)$ is the set of vertices adjacent to v in G. We define the *closure* of A_0 under r-neighbor bootstrap percolation to be $[A_0] = \bigcup_{t=0}^{\infty} A_t$. We say that A_0 *percolates* or is *lethal* if $[A_0] = V(G)$. We define the smallest percolating set on a graph G under r-neighbor bootstrap percolation by the quantity $m(G, r)$. We note that under these rules, it is not possible for vertices to become uninfected.

While it is possible to study bootstrap percolation on any graph G, most contemporary research focuses on multidimensional grids [**?**]. We therefore introduce the following notation. For all $n \in \mathbb{N}$, let $[n] = \{1, 2, \ldots, n\}$. Let the grid graph with vertex set $\prod_i^d [a_i]$ be denoted by $\prod_i^d [a_i]$. Note that $\prod_i^d [a_i] = P_{a_1} \square \cdots \square P_{a_d}$. Furthermore, define:

$$m(a_1, \ldots, a_d, r) = m(\prod_i^d [a_i], r).$$

There are a number of natural generalizations of the problem posed in Question 1. In this thesis, we discuss those obtained by varying the structure of G and the value of r. Below, we outline some of the existing results for graphs that are the Cartesian product of paths and cycles, and $r \in \{0, 1, 2, 3\}$. These results are summarized in Table 1.1.

r	Grids								
	$[a_1]$	$[a_1] \times [a_2]$	$[n]^2$	$[a_1] \times [a_2] \times [a_3]$	$[n]^3$	$\cdots$	$\prod_{i=1}^{d} [a_i]$	$[n]^d$	$[2]^d$
$r = 0$	0	0	0	0	0		0	0	0
$r = 1$	1	1	1	1	1		1	1	1
$r = 2$	$\lceil \frac{a_1-1}{2} \rceil + 1$	$\lceil \frac{a_1+a_2-2}{2} \rceil + 1$	n	$\lceil \frac{a_1+a_2+a_3-3}{2} \rceil + 1$	$\left\lceil \frac{3(n-1)}{2} \right\rceil + 1$		$\left\lceil \frac{\sum_{i=1}^{d}(a_i-1)}{2} \right\rceil + 1$	$\left\lceil \frac{d(n-1)}{2} \right\rceil + 1$	$\lceil \frac{d}{2} \rceil + 1$
$r = 3$	**???**	**???**	$\lceil \frac{n^2+2n+4}{3} \rceil^*$	**S.A. bound**	n^2		**???**	**???**	$\lceil \frac{d(d+3)}{6} \rceil$
$\vdots$						$\ddots$			
$r = d$	**???**	**???**	**???**	**???**	**???**		S.A. bound	n^{d-1}	**???**

Table 1.1: A summary of known bootstrap percolation results for grids and the torus, $r \in \{0, 1, 2, 3, d\}$.

1.1.1 Results on grids and tori

In this section, we highlight major bootstrap percolation results on grids and tori. Some of the following bounds are not tight and require supplemental constructions, which are often difficult to obtain. We further sub-divide this discussion into results on the grid (of which there are many), and results on the torus (of which there are few).

Grids

From the puzzle posed in Question 1, we readily obtain variant problems by altering three parameters: the size and shape of the grid G, the grid's dimension d, and the threshold number of neighbors r. We examine each of these problems in turn.

In the prior discussion of the perimeter argument, we showed that for square grids $[n]^2$, $m([n]^2, 2) \geq n$, and verified this to be tight with a diagonal construction. The following result (attributed to Pete) generalizes this result to all rectangular grids $[a_1] \times [a_2]$. A proof is included for completeness.

Theorem 1.1. *For* $a_1, a_2 \geq 1$,

$$m(a_1, a_2, 2) = \left\lceil \frac{a_1 + a_2 - 2}{2} \right\rceil + 1.$$

Proof. We obtain a lower bound on $m(a_1, a_2, 2)$ by applying the perimeter argument. Note that the perimeter of the $a_1 \times a_2$ grid is $2(a_1 + a_2)$, and so the $m(a_1, a_2, 2) \geq \left\lceil \frac{a_1+a_2}{2} \right\rceil$. (We take the ceiling because the size of infected sets must be integral. See Figure 1.4.) For the upper bound, we proceed by induction on $a_1 + a_2$. For $a_1 + a_2 \leq 4$, the lethal sets in Figure 1.3 match the lower bounds given by the perimeter argument (1, 2, 2, and 2, respectively). For $a_1 + a_2 > 4$, suppose without loss of generality that $a_1 \leq a_2$, and so $a_2 \geq 3$. By hypothesis, $[a_1] \times [a_2 - 2]$ admits a lethal set A_0 at the perimeter bound. We show that A_0, plus the addition of any infection in the final column of $[a_1] \times [a_2]$, is lethal and matches the perimeter bound.

Figure 1.3: Tight constructions for lethal sets where $a_1 + a_2 \leq 4$.

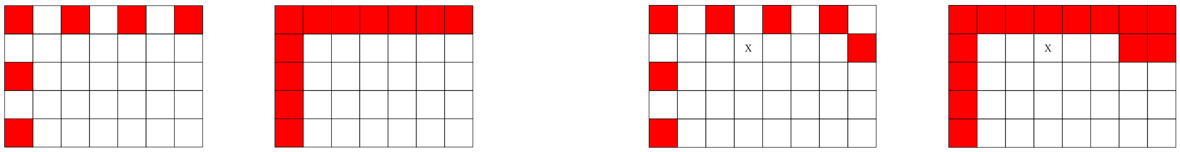

(a) $a + b \equiv 0 \pmod 2$ (b) $a + b \equiv 1 \pmod 2$

Figure 1.4: Tight constructions for lethal sets on the $[a] \times [b]$ grid.

Observe that A_0 infects all vertices of $[a_1] \times [a_2]$, apart from the final two columns. The additional vertex in the final column is then sufficient to infect all remaining healthy vertices. Finally, by incrementing a_2 by two, the perimeter bound is incremented by exactly one. This completes the proof. $\square$

Let us take a moment to examine the issue of integrality in the perimeter bound. Non-integrality occurs either when adjacent vertices are infected in the same generation, or when a vertex is infected by more than r neighbors. Note that in both cases, this decreases the perimeter of infection. One way to think about this is to consider each vertex as having "infectious potential": vertices $v \in A_0$ can infect up to $d(v)$ healthy vertices, whereas vertices $v \in A_i$ for $i > 0$ can infect at most $d(v) - r$. An integral perimeter bound mandates that each vertex realize its potential, whereas a non-integral bound leaves a small margin for error. Figure 1.4a illustrates the integral case, where each cell is infected by exactly two neighboring cells; this condition ensures that $P(A_i) = P([A_0])$ for all i. Conversely, in Figure 1.4b, the cell demarcated with an "X" experiences infection on three sides, thereby reducing its infectious potential. The existence of such a cell is guaranteed by the fact the perimeter bound in this case is non-integral.

We can further generalize for the case of $r = 2$. In 2006, Balogh and Bollobas [1] proved the following general form of Theorem 1.1 for all d-dimensional hypercubes $(a_1, \ldots, a_d)$, $a_i \geq 1$:

Theorem 1.2 (Balogh)**.** *For $d \geq 1$ and $a_1, \ldots, a_d \geq 1$,*

$$m(a_1, \ldots, a_d, 2) = \left\lceil \frac{\sum_{i=1}^{d}(a_i - 1)}{2} \right\rceil + 1.$$

Theorem 1.2 completes the picture for infections with a threshold of two on grids. The next question is whether similar results exist for larger r. Unfortunately, while generalizing to d-dimensional grids yields nice results for $r = 2$, attempts to obtain a holistic understanding of $m(a_1, \ldots, a_d, r)$ for arbitrary r have been largely fruitless. Even the case of $r = 3$ remains stubbornly inaccessible for nearly all large d. However, certain breakthroughs have been made in the following circumstances: $d = 2$, $d = 3$, and $G = [2]^d$.

We first consider 3-neighbor percolation on two-dimensional square grids. In 2021, Benevides et al. proved that

$$m(n, n, 3) = \left\lceil \frac{n^2 + 2n + 4}{3} \right\rceil$$

for even n, and

$$\left\lceil \frac{n^2 + 2n}{3} \right\rceil \leq m(n, n, 3) \leq \left\lceil \frac{n^2 + 2n}{3} \right\rceil + 1$$

for odd n. Additionally, they showed that these bounds are tight for odd n: if $n = 5 \pmod 6$, or $n = 2^k - 1$ for some $k \in \mathbb{N}$, then $m(n, n, 3) = \lceil \frac{n^2+2n}{3} \rceil$; and if $n \in \{9, 13\}$, then $m(n, n, 3) = \lceil \frac{n^2+2n}{3} \rceil + 1$. Constructions that achieve this bound are illustrated in Chapter 7. We add to this picture with the following theorem, proven in Chapter 6, and corollary:

Theorem 1.3. *Suppose that $a, b \geq 1$ such that*

$$m(a, b, 3) = \frac{2ab + a + b}{3}.$$

Then there exists $k \geq 1$ such that $a = b = 2^k - 1$.

Corollary 1.4. *For all $n \geq 1$,*

$$m(n, n, 3) = \begin{cases} \left\lceil \frac{n^2+2n+4}{3} \right\rceil & n \equiv 0 \pmod 2 \\ \frac{n^2+2n}{3} & n = 2^k - 1,\ k \in \mathbb{N} \\ \frac{n^2+2n+1}{3} & n \equiv 5 \pmod 6 \\ \frac{n^2+2n+3}{3} & \textit{otherwise.} \end{cases}$$

Proof. The first three cases follow from Theorem 1 of [?] and the observation that if $n \equiv 5 \pmod 6$, then $\lceil \frac{n^2+2n}{3} \rceil = \frac{n^2+2n+1}{3}$. In the final case, n is congruent to either 1 or 3 modulo 6. This implies that $n^2 + 2n$ is divisible by three. From Theorem 1 of [?], we have that $m(n, n, 3) \leq \frac{n^2+2n+3}{3}$. Furthermore, since n is not of the form $2^k - 1$, it follows from Theorem 1.3 that $m(n, n, 3) > \frac{n^2+2n}{3}$. Therefore, $m(n, n, 3) = \frac{n^2+2n+3}{3}$. □

This result resolves the question of the minimum lethal set for two dimensional square grids. For the more general case of rectangular grids, the problem remains unsolved. However, we are able to achieve an upper bound of $m(a, b, 3) \leq \lceil \frac{ab+a+b+6}{3} \rceil$

and a lower bound (described below) of $m(a,b,3) \geq \lceil \frac{ab+a+b}{3} \rceil$, for all $a, b > 1$. Further discussion of these results can be found in Chapter 6.

One significant and well-known result for 3-neighbor percolation on two- and three-dimensional grids is the following lower bound, taken as a three-dimensional analogue of the perimeter bound. This result is referenced frequently throughout this document, and referred to interchangeably as the *surface area* or *SA bound*. We prove the statement in full generality, while noting that we only make use of the case where $d = 3$. We also note that, like the perimeter bound, the following proof belongs to bootstrap percolation folklore, and appears to have been first published in 1997 by Balogh and Pete [**?**].

Theorem 1.5. *For any $d \geq 1$ and $a_1, a_2, \ldots, a_d \geq 1$,*

$$m(a_1, a_2, \ldots, a_d, d) \geq \frac{\sum_{j=1}^{d} \prod_{i \neq j} a_i}{d}.$$

Proof. We apply the same invariant strategy presented in the perimeter argument. For simplicity, consider $\prod_{i=1}^{d}[a_i]$ to be embedded within the larger graph $\prod_{i=1}^{d}\{0, \ldots, a_i + 1\}$. Note that in $\prod_{i=1}^{d}\{0, \ldots, a_i + 1\}$, each vertex $v \in \prod_{i=1}^{d}[a_i]$ has degree $2d$. Let A_0 be a lethal set in $\prod_{i=1}^{d}[a_i]$ under the d-neighbor bootstrap process. Let A_t be the set of infected vertices in $\prod_{i=1}^{d}[a_i]$ at generation t. Denote by m_t the number of edges between vertices $u \in A_t$ and $v \in \prod_{i=1}^{d}[a_i] \setminus A_t$. We show that $m_{t-1} \geq m_t$ for all $t > 0$.

By definition, each vertex $v \in A_t \setminus A_{t-1}$ has at least d neighbors in A_{t-1}. Therefore, since $d(v) = 2d$, v has no more than d neighbors outside of A_t. This implies that the number of edges from $A_{t-1} \cup \{v\}$ to $\prod_{i=1}^{d}[a_i] \setminus A_{t-1} \cup \{v\}$ cannot exceed m_{t-1}. Furthermore, this holds for every vertex $v \in A_{t-1}$, and so $m_{t-1} \geq m_t$.

Since A_0 is lethal, we have that

$$2d|A_0| \geq m_0 \geq m_1 \geq \cdots \geq 2 \sum_{j=1}^{d} \prod_{i \neq j} a_i,$$

where the final expression gives the total number of edges between the fully infected grid and the surrounding larger grid. Dividing through by $2d$ gives the result. $\square$

We note that the prior argument is precisely the same as the so-called perimeter argument outlined on Page 2. Here, the quantity m_t is a d-dimensional analogue of the perimeter of infection $P(A_t)$ at time-step t, and the lower bound

$$2 \sum_{j=1}^{d} \prod_{i \neq j} a_i$$

is the d-dimensional "perimeter" of the grid. Again, observe that equality can only be obtained when no vertices of A_0 are adjacent, and all vertices $v \in A_{t>0}$ are infected by exactly d neighbors. Any imprecision causes a reduction in "perimeter" of two units, corresponding to a $1/d$ increase in the bound.

The primary aim of this thesis is to prove that the surface area bound is tight for sufficiently large grids when $r = 3$. This process employs a number of general constructions (discussed in Chapter 7), as well as a recursive strategy (Chapter 3). In Chapter 5, we prove the following result:

Theorem 1.6. *For all $a_1, a_2, a_3 \geq 11$,*

$$m(a_1, a_2, a_3, 3) = \left\lceil \frac{a_1 a_2 + a_2 a_3 + a_1 a_3}{3} \right\rceil.$$

Unfortunately, the complete resolution of the $r = 3$ case on grids remains elusive. Tight constructions exist for cubes $[n]^3$ and hypercubes $[2]^d$, but in general bounds are difficult to obtain. Worse, for $r > 3$, the only additional result beyond the surface area bound addresses the very specific case of r-dimensional cubes. Open problems abound.

Tori

In addition to varying the parameters r and d, we might also change the very structure of G. It is natural to shift from grids (the Cartesian product of paths) to tori (the Cartesian product of cycles). In fact, it could be argued that bootstrap percolation on the torus is *more* natural than the grid, since tori are regular and grids are not. This problem has been studied by Benevides et al. In 2021, they obtained the following lower bound for the Cartesian product of two cycles [**?**]. Their proof is included here for completeness.

Theorem 1.7. *For $a, b \geq 1$,*

$$m(C_a \square C_b, 3) \geq \left\lceil \frac{ab + 1}{3} \right\rceil.$$

Proof. Let $G = C_a \square C_b$, and let I be a lethal set on G. Let $H = V(G) \setminus I$, and note that $|H| = ab - |I|$. Let m_H be the number of edges in the subgraph of G induced by H, and m_{IH} be the number of edges between vertices in I and vertices in H. Note that m_{IH} is similar to the notion of perimeter on a grid.

Observe that $G[H]$ must be cycle-free: cycles in $G[H]$ constitute immune regions, and contradict the lethality of I. Therefore, $G[H]$ is a forest, and so $m_H = |H| - c$, where c is the number of components in $G[H]$. Additionally, note that $m_{IH} \leq 4|I|$, since G is 4-regular. Finally, observe that the total degree of $G[H]$ is $2m_H = 4|H| - m_{IH}$.

Chaining together these inequalities, we obtain:

$$\begin{aligned} 4|I| \geq m_{IH} &= 4|H| - 2m_H \\ &= 4|H| - 2(|H| - c) = 2|H| + 2c \\ &= 2(ab - |I|) + 2c \end{aligned}$$

Combining like terms and simplifying, we have

$$|I| \geq \frac{ab+c}{3} \geq \frac{ab+1}{3}.$$

□

Observe that the conditions $c \geq 1$ and $m_{IH} \leq 4|I|$ prevent us from obtaining strict equality. Specifically, if I is lethal, $G[H]$ has one component, and no vertices in I are adjacent, then $|I|$ is minimized. Note that these conditions are quite similar to those on grids; the specific difference is that equality in the bound on grids mandates that no vertex be infected by more than r neighbors, whereas equality on three-dimensional tori requires this inefficiency be centered on one particular vertex.

1.2 Other Problems

In this section, we provide a cursory overview of some other related areas of study in bootstrap percolation. We highlight problems regarding the number of iterations necessary to infect all vertices on a graph.

1.3 Structure of this Thesis

As stated by Theorem 1.6, the primary goal of this thesis is to prove a tight bound for 3-neighbor bootstrap percolation on three-dimensional grids of sufficiently large size. This task requires the use of two major lemmas, as well as both original and previously published ideas and constructions. In an effort to present this material in a coherent manner, the paper is structured as follows.

Chapters 2 and 3 are dedicated to building a conceptual and intuitive framework upon which to prove Theorem 1.6. In Chapter 2, we categorize and present percolating sets on both divisible and non-divisible grids, and discuss the differences between these cases. In Chapter 3, we prove two lemmas allowing us to develop large families of lethal sets that match the surface area bound.

Chapters 4 and 5 leverage the results of Chapter 3 to prove Theorem 1.6. In Chapter 4, we show that all divisible grids (a_1, a_2, a_3), $a_1 \leq a_2 \leq a_3$ admit lethal sets matching the SA bound, and in Chapter 5, we extend this result to all grids of size 11. Chapter

6 further builds on this, highlighting some new results for 3-neighbor percolation on grids of the form $(a_1, a_2, 1)$.

Chapter 7 proves the constructions presented in Chapter 2.

Finally, Chapters 8, 9 and 10 wrap up the discussion with a summary of the programmatic techniques used to discover lethal sets, helpful software resources for future research, how the results of this thesis may be helpful in pursuit of results on the torus, and recommendations for future research in similar and related problems.

Chapter 2
Conceptual Tools

As suggested in Chapter 1, it appears that lethal sets in grid graphs adhere to certain fixed rules. We examine these rules here, and explain why they are necessary and helpful for understanding the problem of bootstrap percolation.

2.1 The d-walls lemma

While it is difficult to identify specific patterns across all lethal sets A_0 under the r-neighbor bootstrap process, there are certain structures that appear frequently enough to warrant discussion. Of particular utility is the following lemma, which states precisely what it means for a set to span a grid (as we saw in Figure 1.2).

Lemma 2.1. *Let A_0 be an infected set on $G = \prod_{i=1}^{d}[a_i]$. Let $\overline{A_0} = V(G) \setminus A_0$, and let $H = G[\overline{A_0}]$ be the subgraph of G induced by $\overline{A_0}$. For $1 \leq k \leq a_j$, let $F_{j,k} = \prod_{i=1}^{j-1}[a_i] \times \{k\} \times \prod_{i=j+1}^{d}[a_i]$ be the kth level of G in the jth dimension. If H does not contain a path between $F_{j,1}$ and F_{j,a_j}, for all $1 \leq j \leq d$, then A_0 is lethal on G under d-neighbor percolation.*

Proof. We proceed by induction on $|V(H)| = \prod_{i=1}^{d} a_i - |A_0|$. If $|V(H)| = 0$, then all vertices of G are infected and we are done. Suppose $|V(H)| > 0$, and consider a connected component Y of H. By hypothesis, for all $j \in [d]$, either $V(Y) \cap F_{j,1} = \emptyset$ or $V(Y) \cap F_{j,a_j} = \emptyset$ (or both). Suppose, without loss of generality, that $V(Y) \cap F_{j,a_j} = \emptyset$. For each $j \in [d]$, let x_j be the maximum value such that $V(Y) \cap F_{j,x_j}$ is non-empty. Note that such an x_j must exist since $|V(H)| > 0$.

Consider the vertex $\vec{x} = (x_1, \ldots, x_d) \in V(Y)$, and observe that

$$\{\bigcup_{j \in [d]} F_{j,x_j+1}\} \cap V(Y) = \emptyset.$$

In particular, note that $(x_1 + 1, x_2, \ldots, x_d), \ldots, (x_1, \ldots, x_d + 1) \in N_S(\vec{x})$. Therefore, $\vec{x}$ becomes infected. Furthermore, since $|V(H) \setminus \{\vec{x}\}| < |V(H)|$, the resulting graph percolates by induction. This completes the proof. $\square$

Corollary 2.2. *Let G be the grid graph $\prod_{i=1}^{d}[a_i]$. For each $j \in [d]$ and some $1 \leq k \leq a_j$, let*

$$M = \bigcup_{j,k} F_{j,k}$$

be a subset of the vertices of G formed by the union of mutually orthogonal faces. If a set A_0 is lethal on M, then it is lethal on G.

Proof. Since A_0 is lethal on M, there exists a time t where $M \subseteq A_t$. Therefore, for all $j \in [d]$, the graph $G[\overline{A_t}]$ cannot contain a path between $F_{j,1}$ and F_{j,a_j}. By Lemma 2.1, A_0 is lethal on G. □

Corollary 2.2 provides a general description of lethal sets on d-dimensional grids in terms of their $(d-1)$-dimensional faces, provided these faces are mutually orthogonal. Here, we return to the notion first introduced in Chapter 1 of the capacity of a lethal set to span a grid. In particular, we see that the set in Figure 1.2a is comprised of lethal sets under the 2-neighbor bootstrap process on the two one-dimensional orthogonal faces $F_{1,1}$ and $F_{2,1}$ of $[10]^2$. In this regard, the problem of obtaining perfect d-neighbor lethal sets on d-dimensional grids is reduced to the problem of determining a "good" union M of mutually orthogonal $(d-1)$-dimensional faces. In Chapter 7, we apply this idea to obtain an infinite family of three-dimensional grids from three orthogonal two-dimensional faces. However, we caution that the challenge of determining a "good" union M is non-trivial in general.

The following corollary (taken as a particular instance of Corollary 2.2) will be useful in our discussion of lethal sets on three-dimensional grids (a_1, a_2, a_3).

Corollary 2.3. *Let G be the grid graph (a_1, a_2, a_3). If a set A_0 is lethal on $F_{1,1} \cup F_{2,1} \cup F_{3,1}$, then A_0 is lethal on G.*

Proof. By hypothesis, A_0 is lethal on $F_{1,1} \cup F_{2,1} \cup F_{3,1}$. Therefore, there exists some time t for which $F_{1,1} \cup F_{2,1} \cup F_{3,1} \subseteq A_t$, and so $G[\overline{A_t}]$ satisfies the conditions of Lemma 2.1. We conclude that A_0 is lethal on G. □

In the case of three-dimensional grids, it is instructive to think of the perpendicular faces $M = F_{1,1} \cup F_{2,1} \cup F_{3,1}$ as an unfolded surface (see Figure 2.1). We refer to M as a manifold of G, and to this unfolded surface as a *proper unfolding* of M. In Chapter 7, we examine other manifolds and their proper unfoldings.

Since, by Corollary 2.2, any lethal set on M is also lethal on G, it is often easier to identify lethal sets by examining these flattened unfolded structures. In fact, in the particular case of $M = F_{1,1} \cup F_{2,1} \cup F_{3,1}$, the surface area bound on (a_1, a_2, a_3) can be written in terms of the surface area bounds on flat, two-dimensional grids.

Lemma 2.4. *For $a_1 \geq a_2 \geq a_3 \geq 1$,*

$$SA(a_1, a_2, a_3) = SA(a_1 + a_3 - 1, a_2 + a_3 - 1, 1) - SA(a_3 - 1, a_3 - 1, 1).$$

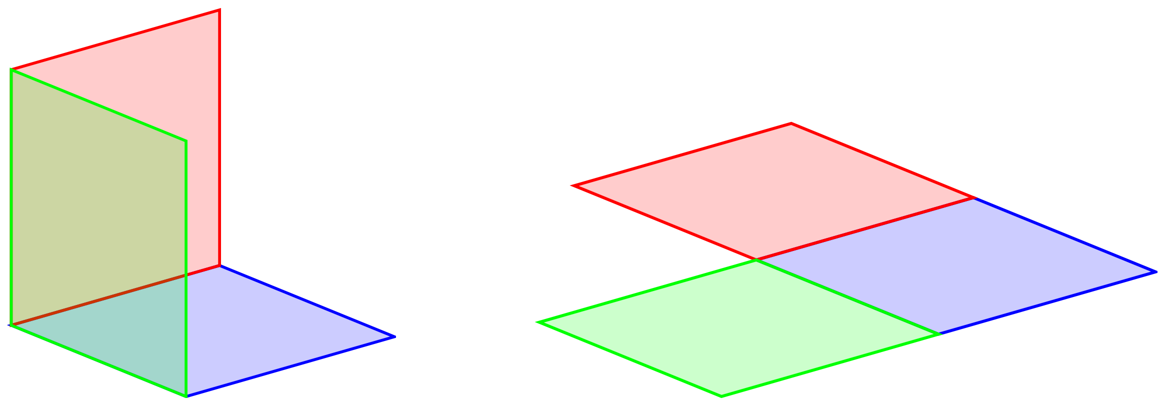

Figure 2.1: Three perpendicular faces of (a_1, a_2, a_3) (left) and their representation as a flat unfolded surface (right).

Proof. Taking the surface area bound on the righthand side of the above equation, we obtain

$$\mathrm{SA}(a_1 + a_3 - 1, a_2 + a_3 - 1, 1) = \frac{a_1a_2 + a_1a_3 + a_2a_3 + a_3^2 - 1}{3}$$

and

$$\mathrm{SA}(a_3 - 1, a_3 - 1, 1) = \frac{a_3^2 - 1}{3}.$$

Adding these two expressions together gives

$$\frac{a_1a_2 + a_1a_3 + a_2a_3}{3},$$

which is precisely the surface area bound for (a_1, a_2, a_3). □

In the context of Figure 2.1, this lemma tells us that a percolating set on the (a_1, a_2, a_3) grid (left of Figure 2.1) is precisely the same size as a percolating set on the complete flattened rectangle minus the size of a percolating set on the missing region (right of Figure 2.1). In practice, this lemma allows us to leverage an understanding of lethal sets on two-dimensional grids to obtain lethal sets in three dimensions. However, care is required in this process, and the existence of an optimal set on a two-dimensional grid does not immediately guarantee the existence of such a set in three dimensions.

2.2 3-neighbor percolation on two-dimensional grids

It is clear that an understanding of the behavior of 3-neighbor percolation on two-dimensional grids is of use in our investigation of 3-neighbor percolation on (a_1, a_2, a_3) grids. In Chapter 6 we examine the problem of 3-neighbor percolation on square two-dimensional grids, and answer a question posed by Benevides et alia regarding the value

mod 3	$a_1 \equiv 0$	$a_1 \equiv 1$	$a_1 \equiv 2$
$a_2 \equiv 0$			
$a_2 \equiv 1$			
$a_2 \equiv 2$			

(a) $a_3 \equiv 1 \pmod 3$

mod 3	$a_1 \equiv 0$	$a_1 \equiv 1$	$a_1 \equiv 2$
$a_2 \equiv 0$			
$a_2 \equiv 1$			
$a_2 \equiv 2$			

(b) $a_3 \equiv 2 \pmod 3$

mod 3	$a_1 \equiv 0$	$a_1 \equiv 1$	$a_1 \equiv 2$
$a_2 \equiv 0$			
$a_2 \equiv 1$			
$a_2 \equiv 2$			

(c) $a_3 \equiv 0 \pmod 3$

Table 2.1: Integrality of grids by congruence class. Green indicates integral surface area bound.

of $m([n]^2, 3)$. Here, we describe some of the structural properties of lethal sets on two-dimensional grids that will prove useful in that analysis. The following propositions are due to Benevides et al [**?**].

Proposition 2.5. *Let A_0 be a lethal set on $[a_1] \times [a_2]$ under 3-neighbor percolation. Then A_0 contains all four corner vertices of $[a_1] \times [a_2]$.*

Proof. Since corner vertices in $[a_1] \times [a_2]$ have degree 2, they cannot become infected. Therefore, since A_0 is lethal, it must contain all corner vertices. □

Proposition 2.6. *Let B be the set of vertices on the border of $[a_1] \times [a_2]$, and let $u, v \in B$ be adjacent vertices. If A_0 is a lethal set under 3-neighbor percolation, then $A_0 \cap \{u, v\} \neq \emptyset$.*

Proof. Assume for contradiction that $A_0 \cap \{u, v\} = \emptyset$. Since u, v are border vertices, $d(u) \leq d(v) \leq 3$. Because A_0 is lethal, u and$v$ must become infected. Suppose, without loss of generality, that u is infected first. This is impossible, since $d(u) \leq 3$ and v is not infected. □

Proposition 2.7. *Let A_0 be a lethal set on $[a_1] \times [a_2]$ under 3-neighbor percolation. Let $H = V([a_1] \times [a_2]) \setminus A_0$. Then the subgraph induced by H is acyclic and each component of H contains at most one border vertex.*

Proof. Suppose for contradiction that C is a cycle in H. Let $v \in C$ be the first vertex of C to become infected. Note that v has two uninfected neighbors in C. Since $d(v) \leq 4$, v cannot become infected, a contradiction.

Suppose P is a path in H with endpoints on the border. No vertex v in P can become infected, since v has at most two neighbors outside of P. □

Proposition 2.7 more clearly articulates the notion of immune regions discussed in Chapter 1. While such immune regions exist in higher-dimensional grids, their structure is substantially harder to define.

It will be insightful to consider the surface area bound on two-dimensional grids in the context of Propositions 2.5, 2.6 and 2.7. For simplicity, we introduce the following terms. We refer to grids with integral surface area bounds as *divisibility cases* and grids with non-integral bounds as *non-divisibility cases*. The divisibility and non-divisibility cases for three-dimensional grids where $r = 3$ are illustrated in Table 2.1. Let $A_0 \subseteq V(G)$ be a lethal set on G that matches the surface area bound. We call A_0 *perfect* if G is a divisibility case, and *optimal* if G is a non-divisibility case.

Recall from Chapter 1 that a lethal initial infection A_0 is perfect if it contains no adjacent vertices, and if all vertices $v \in A_{t>0}$ are infected by precisely d neighbors. Therefore, by Propositions 2.5 and 2.6, if $[a_1] \times [a_2]$ admits a perfect lethal set, then $a_1, a_2 \equiv 1 \pmod 2$. Furthermore, every component of the subgraph H induced by uninfected vertices must contain exactly one border vertex (otherwise the second condition on perfect infections would be violated). In Chapter 6, we use these observations to prove that the only two-dimensional grids that admit perfect lethal sets under 3-neighbor bootstrap percolation are of the form $[2^n - 1]^2$.

2.3 Outline of main result

The proof of Theorem 1.6 relies on the existence of a number of infinite families of perfect lethal sets. These are constructions that match the surface area bound and can be extended in one or two dimensions. Tables 2.2, 2.3 and 2.4 display these families. Proofs of the lethality of these constructions are presented in Chapter 7 and Appendix A.

In the following chapter, we present a technique for recursively assembling small perfect sets into large perfect sets. By repeatedly applying this recursion to the sets illustrated in Tables 2.2, 2.3 and 2.4, we are able to obtain perfect sets for all grids (a_1, a_2, a_3) where $a_1 \geq a_2 \geq a_3 \geq 5$. We extend this result to non-divisibility cases by applying the recursion to a small set of optimal grids illustrated in Appendix A.

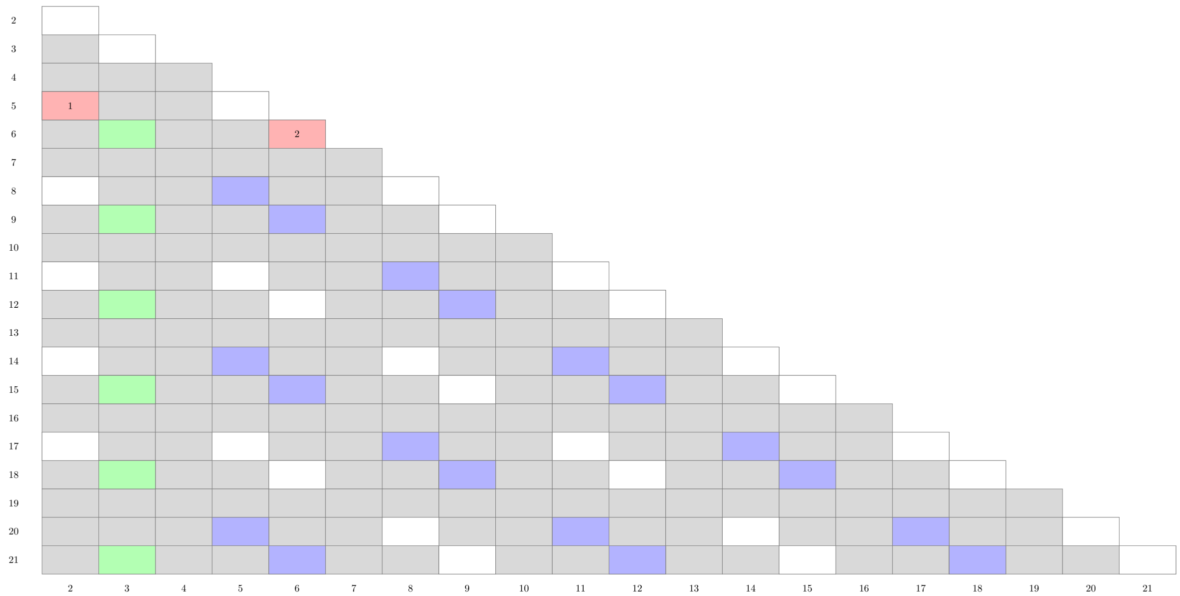

Table 2.2: Necessary thickness 2 constructions for Theorem 1.6. Blue and green cells represent infinite families of constructions. Red cells are individual constructions. Divisibility cases are white and non-divisibility cases are gray.

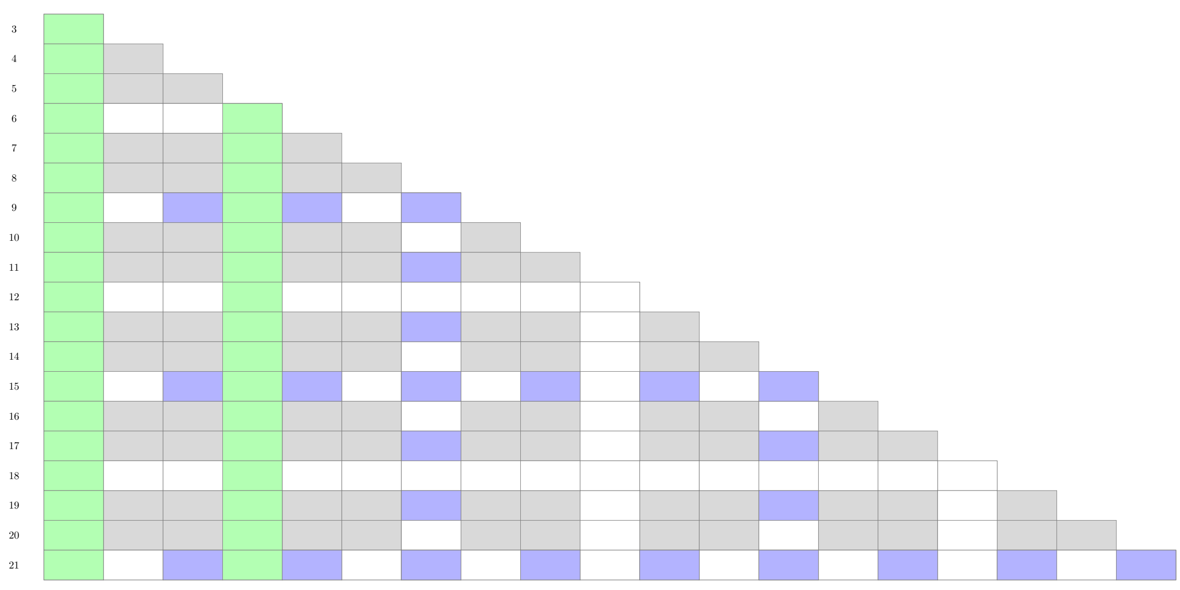

Table 2.3: Necessary thickness 3 constructions for Theorem 1.6. Blue and green cells represent infinite families of constructions. Red cells are individual constructions. Divisibility cases are white and non-divisibility cases are gray.

5	1																
6		3															
7																	
8	2			4													
9																	
10																	
11																	
12																	
13																	
14																	
15																	
16																	
17																	
18																	
19																	
20																	
21																	
	5	6	7	8	9	10	11	12	13	14	15	16	17	18	19	20	21

Table 2.4: Necessary thickness 5 constructions for Theorem 1.6. Blue and green cells represent infinite families of constructions. Red cells are individual constructions. Divisibility cases are white and non-divisibility cases are gray.

Chapter 3
A Recursive Technique

In the previous chapter, we examined some structures in grids that, if present, immediately guarantee lethality. Most significantly, we proved that lethal sets on mutually orthogonal walls of a grid are lethal on the entire grid. In the following sections, we leverage this result to show that certain configurations of fully infected sub-grids (which we shall call blocks) will cause the larger grid to become infected. Furthermore, we show that if each of these smaller blocks is infected with a minimum lethal set, the composite larger brick will also be infected with a minimum lethal set (barring some considerations for divisibility).

The proof of this claim makes use of the so-called *modified bootstrap process* in $[n]^d$, discussed in [**?**] and [**?**]. This is a strengthened variation of the problem introduced in Chapter 1, whereby vertices in the $[n]^d$ grid become infected if and only if they are adjacent to infected vertices along edges in each of the d directions. For example, in the $[n]^2$ grid, a vertex that sees infection in one of both the North/South and East/West directions will itself become infected, whereas a vertex with infected neighbors to the East and West (but not North and South) will not.

In particular, the following lemma considers composite grids $[n]^d$ where each vertex $x = (x_1, \ldots, x_d) \in [n]^d$ is itself a smaller block G_x. We prove that lethal sets on these grids can be built from the smaller lethal sets on each G_x.

Lemma 3.1. *For $n, d \geq 1$, let $A = (a_{i,j})$ be a $d \times n$ matrix of positive integers, and let $b_i = \sum_{j=1}^{n} a_{i,j}$, for $1 \geq j \geq d$. Let S be a lethal set under the modified process on $[n]^d$, and for each vertex $\vec{x} = (x_1, \ldots, x_v) \in S$, let $T_{\vec{x}}$ be a lethal set on $\prod_{i=1}^{d}[a_{i,x_i}]$ under d-neighbor percolation. Then*

$$m(b_1, \ldots, b_d, d) \leq \sum_{\vec{x} \in S} |T_{\vec{x}}|.$$

Proof. We imagine sub-dividing the $\prod_{i=1}^{d}[b_i]$ brick into smaller blocks by partitioning each of the d axes into segments $a_{i,1}, a_{i,2}, \ldots, a_{i,n}$, $1 \leq i \leq d$. Each block is given by a unique product of these segments, and represented by a vector $\vec{x} = (x_1, \ldots, x_d) \in [n]^d$.

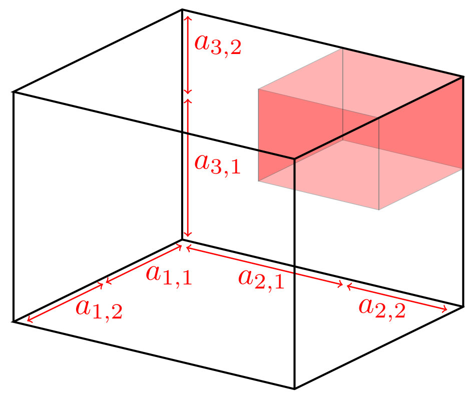

Figure 3.1: A recursively constructed $[b_1] \times [b_2] \times [b_3]$ grid, for $n = 2$, $d = 3$.

Formally, for each such $\vec{x}$, let $G_{\vec{x}}$ be the block with vertex set

$$\prod_{i=1}^{d} \{1 + \sum_{j=1}^{x_i - 1} a_{i,j}, \ldots, \sum_{j=1}^{x_i} a_{i,j}\},$$

and edges between vertices that differ by one in exactly one coordinate. Figure 3.1 illustrates the block $G_{\vec{x}}$ for $\vec{x} = (1, 2, 2) \in [2]^3$. Observe that $G_{\vec{x}}$ is isomorphic to $\prod_{i=1}^{d} [a_{i,x_i}]$.

For each $\vec{x} \in S$, let $A_{\vec{x}}$ be the vertices of $G_{\vec{x}}$ corresponding to the vertices of $T_{\vec{x}}$ under isomorphism from $\prod_{i=1}^{d} [a_{i,x_i}]$ to $G_{\vec{x}}$, and let $A_0 = \cup A_{\vec{x}}$. Observe that $|A_0| = \sum_{\vec{x} \in S} |T_{\vec{x}}|$. We show that A_0 is lethal on $\prod_{i=1}^{d} [b_i]$.

By the definition of $T_{\vec{x}}$, for each $\vec{x} \in S$, $A_{\vec{x}}$ is lethal on $G_{\vec{x}}$. Imagine running the d-neighbor process until all blocks $G_{\vec{x}}$ are fully infected. We claim that this is sufficient to infect all remaining vertices of $\prod_{i=1}^{d} [b_i]$. Consider the remaining blocks $G_{\vec{x}}$, for $\vec{x} \in [n]^d \setminus S$. Since S is lethal under the modified process, each $G_{\vec{x}}$ is adjacent to fully infected blocks in all d directions. In particular, if we consider expanding out the faces of $G_{\vec{x}}$ towards these infected blocks, the resulting cube has d fully infected faces that share a common corner. By Corollary 2.3, this structure will infect all the vertices of $G_{\vec{x}}$. Repeating this process on each uninfected region of $\prod_{i=1}^{d} [b_i]$ (as they are exposed under the modified process) ultimately results in all vertices becoming infected. This completes the proof. □

We note that although the lemma above is true in full generality, we are only concerned with the particular case where $n = 2$ and $d = 3$. The following corollary proves that the bound in Lemma 3.1 is tight for $n = 2$ and $d = 3$, if lethal sets on at least three of the constituent blocks are perfect.

Corollary 3.2. *Let $A = (a_{i,j})$ be a 3×2 matrix of positive integers, and let $b_i = a_{i,1} + a_{i,2}$*

for all $1 \leq i \leq 3$*. Then* $m(b_1, b_2, b_3, 3)$ *is at most*

$$m(a_{1,1}, a_{2,1}, a_{3,1}, 3) + m(a_{1,2}, a_{2,2}, a_{3,1}, 3) + m(a_{1,2}, a_{2,1}, a_{3,2}, 3) + m(a_{1,1}, a_{2,2}, a_{3,2}, 3).$$

Furthermore, this bound is tight if at least 3 of the constituent grids are perfect.

Proof. The upper bound on $m(b_1, b_2, b_3, 3)$ is a direct consequence of Lemma 3.1, since $(1,1,1), (2,2,1), (2,1,2), (1,2,2)$ is lethal under the modified process on $[2]^3$.

If all grids are perfect, then:

$$\begin{aligned}
&m(a_{1,1}, a_{2,1}, a_{3,1}, 3) + m(a_{1,2}, a_{2,2}, a_{3,1}, 3) + m(a_{1,2}, a_{2,1}, a_{3,2}, 3) + m(a_{1,1}, a_{2,2}, a_{3,2}, 3)\\
&= \frac{a_{1,1}a_{2,1} + a_{2,1}a_{3,1} + a_{3,1}a_{1,1}}{3} + \frac{a_{1,2}a_{2,2} + a_{2,2}a_{3,1} + a_{3,1}a_{1,2}}{3}\\
&\qquad + \frac{a_{1,2}a_{2,1} + a_{2,1}a_{3,2} + a_{3,2}a_{2,1}}{3} + \frac{a_{1,1}a_{2,2} + a_{2,2}a_{3,2} + a_{3,2}a_{1,1}}{3}\\
&= \frac{(a_{1,1} + a_{1,2})(a_{2,1} + a_{2,2}) + (a_{2,1} + a_{2,2})(a_{3,1} + a_{3,2}) + (a_{3,1} + a_{3,2})(a_{1,1} + a_{1,2})}{3}\\
&= \frac{b_1b_2 + b_2b_3 + b_3b_1}{3}.
\end{aligned}$$

Similarly, suppose, without loss of generality, that $(a_{1,1}, a_{2,1}, a_{3,1})$ is optimal and the remaining grids are perfect. Then:

$$\begin{aligned}
&m(a_{1,1}, a_{2,1}, a_{3,1}, 3) + m(a_{1,2}, a_{2,2}, a_{3,1}, 3) + m(a_{1,2}, a_{2,1}, a_{3,2}, 3) + m(a_{1,1}, a_{2,2}, a_{3,2}, 3)\\
&= \left\lceil \frac{a_{1,1}a_{2,1} + a_{2,1}a_{3,1} + a_{3,1}a_{1,1}}{3} \right\rceil + \frac{a_{1,2}a_{2,2} + a_{2,2}a_{3,1} + a_{3,1}a_{1,2}}{3}\\
&\qquad + \frac{a_{1,2}a_{2,1} + a_{2,1}a_{3,2} + a_{3,2}a_{2,1}}{3} + \frac{a_{1,1}a_{2,2} + a_{2,2}a_{3,2} + a_{3,2}a_{1,1}}{3}\\
&= \left\lceil \frac{(a_{1,1} + a_{1,2})(a_{2,1} + a_{2,2}) + (a_{2,1} + a_{2,2})(a_{3,1} + a_{3,2}) + (a_{3,1} + a_{3,2})(a_{1,1} + a_{1,2})}{3} \right\rceil\\
&= \left\lceil \frac{b_1b_2 + b_2b_3 + b_3b_1}{3} \right\rceil.
\end{aligned}$$

In both cases, we obtain the lower bound $m(b_1, b_2, b_3, 3)$. This completes the proof. □

3.1 Applying the recursion

Corollary 3.2 provides a perscriptive method for constructing optimal and perfect lethal sets recursively, provided the existence of sufficiently many small building blocks. In the following chapter, we use this technique to obtain perfect lethal sets on all (b_1, b_2, b_3) grids, for $b_1, b_2, b_3 \geq 5$, and optimal lethal sets on all (b_1, b_2, b_3) grids, for $b_1, b_2, b_3 \geq 11$. To facilitate this process, we first present some useful constructions of lethal sets (discussed in greater detail in Chapter [Constructions]), as well as particular applications of Corollary 3.2 that hold for general grids.

Proposition 3.3. *For all $k \geq 1$ such that $k \neq 2$, $(3, 3, k)$ is perfect.*

Proposition 3.4. *For all $k \geq 2$, $(3, 6, k)$ is perfect.*

Proposition 3.5. *For all $k \equiv 3 \pmod 6$ and $l \equiv 1 \pmod 2$ such that $l > 1$, $(3, k, l)$ is perfect.*

Proposition 3.6. *For all $k, l \in \{2, 5\} \pmod 6$ such that $k \not\equiv 7 \pmod 6$ and $k, l > 2$, $(k, l, 2)$ is perfect.*

Proposition 3.7. *For all $k \equiv 3 \pmod 6$, $(k, 4, 3)$ is perfect.*

Combining the above propositions with Corollary 3.2, we are able to obtain the following lemmas.

Lemma 3.8. *Suppose (b_1, b_2, b_3) is optimal. Then $(b_1 + 3, b_2 + 3, b_3 + 3)$ is optimal.*

Proof. By Proposition 3.3, each of $(b_1, 3, 3), (3, b_2, 3), (3, 3, b_3)$ is perfect. Therefore, by Corollary 3.2,

$$m(b_1+3, b_2+3, b_3+3, 3) = m(b_1, b_2, b_3, 3) + m(b_1, 3, 3, 3) + m(3, b_2, 3, 3) + m(3, 3, b_3, 3),$$

and so $(b_1 + 3, b_2 + 3, b_3 + 3)$ is optimal. □

3.2 Examples and Notation

3.3 Regional vs. Temporal Infections

Chapter 4
A Tight Bound on Grids of Size ≥ 5

4.1 Introduction and Definitions

Let the ordered tuple (a, b, c) represent the $a \times b \times c$ grid G where $a \geq b \geq c$. We refer to c as the *thickness* of G. For example, the tuple $(5, 3, 3)$ represents a $5 \times 3 \times 3$ grid of thickness 3. We refer to a tuple as *divisible*, or a *divisibility case*, if and only if $ab + bc + ca \equiv 0 \pmod 3$. If a tuple is divisible and percolates at the lower bound, we refer to it as *perfect*. Observe that the divisibility cases are precisely those grids with integral lower bounds. The divisibility cases of thicknesses belonging to the three residue classes modulo 3 are illustrated in {Figure something}.

In the following lemmas, we use the notation $(a, b, c)+(x, y, z) = (a+x, b+y, c+z)$ to represent respective increases of x, y, and z to the side lengths a, b, and c of G. We note the following:

Remark 4.1. By applying the recursion, $(a, b, c) + (x, y, z)$ percolates at the lower bound when either:

1. $(a, b, c), (a, y, z), (x, b, z), (x, y, c)$ all percolate at the lower bound; or

2. $(x, y, z), (x, b, c), (a, y, c), (a, b, z)$ all percolate at the lower bound.

We shall call a thickness *complete* if it can be shown that all divisibility cases in that thickness are perfect. In this section, we demonstrate that thickness 5, thickness 6 and thickness 7 are all complete. As these belong to the residue classes 2, 0, and 1 modulo 3, respectively, we then use a recursive construction to show that all larger grids are also complete.

4.2 Completeness of Thickness 5

Leveraging {lemmas from earlier chapters yet to be written}, we show that all divisibility cases in thickness 5 percolate at the lower bound.

NOTE: THE FOLLOWING LEMMAS HOLD ASSUMING WE HAVE A GENERAL CONSTRUCTION FOR $(2,3,3k)$ FOR ALL k.

Lemma 4.2. *All divisibility cases for grids of the form $(k,5,5)$ are perfect.*

Proof. We consider grids obtained from $(5,2,2)+(a,3,3)$, for $a \equiv 0 \pmod 3$ and $a>3$. By remark 4.1, it is sufficient to show that $(5,2,2),(5,3,3),(a,2,3),(a,2,3)$ are all perfect. By {a bunch of constructions}, each of these grids percolates at the lower bound for $a>3$. We therefore obtain all grids of the form $(k,5,5)$, for $k>8$. The only missing grids are $(5,5,5)$ and $(8,5,5)$, which we have by construction. This completes the proof. □

Lemma 4.3. *All divisibility cases for grids of the form $(k,6,5)$ percolate at the lower bound.*

Proof. We consider grids obtained from $(6,3,2)+(a,3,3)$, for $a \equiv 0 \pmod 3$ and $a>3$. By remark 4.1, it is sufficient to show that $(6,3,2),(6,3,3),(a,3,3),(a,3,2)$ are all perfect. By {a bunch of constructions}, each of these grids percolates at the lower bound for $a>3$. We therefore obtain all grids of the form $(k,6,5)$, for $k>8$. The only missing grid is $(6,6,5)$, which we have by construction. This completes the proof. □

Lemma 4.4. *Thickness 5 is complete.*

Proof. Let $(a,b,2)$ represent an arbitrary (divisible) grid of thickness 2, and let $x=a \pmod 6$ and $y=b \pmod 6$. By {some as of yet unwritten construction}, we have that $(a,b,2)$ percolates at the lower bound for all $x,y\in\{0,2,3,5\}$, where $x\neq y$. We consider two constructions: $(a,b,2)+(6,3,3)$ and $(a,b,2)+(6,6,3)$.

By item (1) of the remark, in order to show that $(a,b,2)+(6,3,3)$ percolates at the lower bound, it is sufficient to show that $(a,b,2),(a,3,3),(6,b,3),(6,3,2)$ all percolate at the bound. By {more unwritten constructions}, this is true for all $x,y\in\{0,2,3,5\}$, where $x\neq y$, $a,b>1$, and at least one of $\{a,b\}>2$. (Note that if $a=2$, one of the tuples is $(2,3,3)$, which does not percolate at the lower bound; we accommodate for this by re-writing $(a,b,2)+(6,3,3)$ as $(a,b,2)+(3,6,3)$.) The resulting tuple $(a',b',5)$ is a grid of thickness 5, with a' and b' in the same residue class modulo 6, $x,y\geq 8$, and at least one of $\{a',b'\}\geq 9$. From {some figure representing the divisibility cases of thickness 5}, we see that the lower bound on a' and b' omits all grids of the form $(5,5,k)$ and $(5,6,k)$, as well as the singular grid $(8,8,5)$.

Applying an analogous argument to $(a,b,2)+(6,6,3)$, we must demonstrate that $(a,b,2),(a,6,3),(6,b,3),(6,6,2)$ all percolate at the lower bound. By {some other constructions}, we again find that this holds for all $x,y\in\{0,2,3,5\}$, where $x\neq y$ and $a,b>1$. This gives all thickness 5 tuples $(a',b',5)$ with a' and b' in different residue classes modulo 6, where $a',b'\geq 8$.

	6	7	8	9	10	11	12	13	14	15	16	17	18
6	1												
7	4												
8	1												
9		2	3	2									
10	1			3									
11	4			2									
12	1	4	1		1	4	1						
13	4			2			4						
14	1			3			1						
15		2	3	2	3	2		2	3	2			
16	1			3			1			3			
17	4			2			4			2			
18	1	4	1		1	4	1	4	1		1	4	1

Table 4.1: The four thickness 6 cases analyzed in Lemmas 4.5 (blue), 4.6 (green), 4.7 (red), and 4.8 (yellow).

Combining these results, we have completeness for all grids of thickness 5 except those of the form $(5, 5, k)$ and $(5, 6, k)$, and the singular grid $(8, 8, 5)$. By lemmas 4.2 and 4.3, and {some construction for $(8, 8, 5)$}, these cases are also complete, and so thickness 5 is complete. This completes the proof. $\square$

4.3 Completeness of Thickness 6

We shall show that all grids of thickness 6 can be obtained recursively from $(3n, m, 3)$, where $n, m \equiv 1 \pmod 2$ (this is that general thickness 3 construction), and one of $\{(3, 3, 3), (6, 6, 3), (6, 3, 3), (3, 6, 3)\}$. We examine each of these cases separately and show that each is complete.

(NOTE (to Peter and Jon): I have struggled a bit with the canonical way to describe grids. I like the tuple representation (a, b, c) where WLOG $a \leq b \leq c$. However, this becomes a bit mucky in the following proofs, because $(3n, m, 3)$ potentially violates this rule if n is large and m is small. To accommodate this, I have written "grids of the form $(a, b, 6)$, where $a \equiv 0 \pmod 6$ and $b \equiv 0 \pmod 2$, or $b \equiv 0 \pmod 6$ and $a \equiv 0 \pmod 2$," in an attempt to address the circumstance where the ordering of the tuple is flipped because n is large and m is small. However, I think this may just muddy the waters.)

Lemma 4.5. *All grids of the form $(a, b, 6)$, where $a \equiv 0 \pmod 6$ and $b \equiv 0 \pmod 2$, or $b \equiv 0 \pmod 6$ and $a \equiv 0 \pmod 2$, percolate at the lower bound.*

Proof. We consider $(3n, m, 3) + (3, 3, 3)$, for $n, m \equiv 1 \pmod 2$. By remark 4.1, we have that $(3n, m, 3) + (3, 3, 3)$ percolates if $(3n, m, 3), (3n, 3, 3), (3, m, 3), (3, 3, 3)$ all percolate. By construction {yet to be named}, all grids $(a, 3, 3)$ are perfect. Therefore, $(3, 3n, m) + (3, 3, 3)$ is perfect. Note that this grid is of the form $(3k, l, 6)$, where $k, l \equiv 0 \pmod 2$. This is equivalent to grids of the form $(a, b, 6)$, where $a \equiv 0 \pmod 6$ and $b \equiv 0 \pmod 2$, or $b \equiv 0 \pmod 6$ and $a \equiv 0 \pmod 2$. This completes the proof. □

Lemma 4.6. *All grids of the form $(a, b, 6)$, where $a \equiv 3 \pmod 6$ and $b \equiv 1 \pmod 2$, or $b \equiv 3 \pmod 6$ and $a \equiv 1 \pmod 2$, percolate at the lower bound.*

Proof. We apply the same argument as above, this time considering $(3n, m, 3) + (6, 6, 3)$, for $n, m \equiv 1 \pmod 2$. Again, by remark 4.1, it is sufficient to show that $(3n, m, 3), (3n, 6, 3), (6, m, 3), (6, 6, 3)$ are all perfect. By {more thickness 3 constructions}, each of these grids percolates at the lower bound. The resulting grid, $(3n, m, 3) + (6, 6, 3)$, for $n, m \equiv 1 \pmod 2$, is of the form $(a, b, 6)$, for $a \equiv 3 \pmod 6$ and $b \equiv 1 \pmod 2$, or $b \equiv 3 \pmod 6$ and $a \equiv 1 \pmod 2$. This completes the proof. □

Lemma 4.7. *All grids of the form $(a, b, 6)$, where $a \equiv 3 \pmod 6$ and $b \equiv 0 \pmod 2$, or $b \equiv 3 \pmod 6$ and $a \equiv 0 \pmod 2$, percolate at the lower bound.*

Proof. Similarly to the previous proofs, we consider $(3n, m, 3) + (6, 3, 3)$, for $n, m \equiv 1 \pmod 2$. We show that $(3n, m, 3), (3n, 3, 3), (6, m, 3), (6, 3, 3)$ are all perfect. By the same thickness 3 constructions, each of these grids percolates at the lower bound. Therefore, by remark 4.1, $(3n, m, 3) + (6, 3, 3)$ is perfect. Furthermore, observe that $(3n, m, 3) + (6, 3, 3)$ is of the form $(a, b, 6)$, where $a \equiv 3 \pmod 6$ and $b \equiv 0 \pmod 2$. This completes the proof. □

Lemma 4.8. *All grids of the form $(a, b, 6)$, where $a \equiv 0 \pmod 6$ and $b \equiv 1 \pmod 2$, or $b \equiv 0 \pmod 6$ and $a \equiv 1 \pmod 2$, percolate at the lower bound.*

Proof. We consider $(3n, m, 3) + (3, 6, 3)$, for $n, m \equiv 1 \pmod 2$. We show that $(3n, m, 3)$, $(3n, 6, 3)$, $(3, m, 3), (3, 6, 3)$ are all perfect. By {thickness 3 constructions} and remark 4.1, $(3n, m, 3) + (3, 6, 3)$ is perfect. Observe that $(3n, m, 3) + (3, 6, 3)$ is of the form $(a, b, 6)$, where $a \equiv 0 \pmod 6$ and $b \equiv 1 \pmod 2$. This completes the proof. □

Lemma 4.9. *Thickness 6 is complete.*

Proof. All divisibility cases for thickness 6 are grids of the form $(x, y, 6)$ such that at least one of $\{x, y\}$ is congruent to 0 modulo 3. Lemmas 4.5, 4.6, and 4.7 cover all such cases. The result follows. □

	7	8	9	10	11	12	13	14	15	16	17	18	19
7	1												
8													
9			3										
10	2			1									
11													
12			4			3							
13	1			2			1						
14													
15			3			4			3				
16	2			1			2			1			
17													
18			4			3			4			3	
19	1			2			1			2			1

Table 4.2: The four thickness 7 cases analyzed in Lemmas 4.10 (blue), 4.11 (green), 4.12 (red), and 4.13 (yellow).

4.4 Completeness of Thickness 7

We show that all divisibility cases for grids of thickness 7 admit perfect lethal sets. Observe that divisibility cases for thickness 7 consist of grids of the form $(x, y, 7)$ for x, y in residue classes $\{0, 1, 3, 4\}$ modulo 6 (see Table 4.2). We separate these divisibility cases into the following four categories and show that each category is complete:

1. $(x, y, 7)$ for $x, y \in \{1, 4\}$ and $x \equiv y \pmod 6$;
2. $(x, y, 7)$ for $x, y \in \{1, 4\}$ and $x \not\equiv y \pmod 6$;
3. $(x, y, 7)$ for $x, y \in \{0, 3\}$ and $x \equiv y \pmod 6$;
4. $(x, y, 7)$ for $x, y \in \{0, 3\}$ and $x \not\equiv y \pmod 6$.

Lemma 4.10. *All grids of the form $(x, y, 7)$ for $x, y \in \{1, 4\}$ and $x \equiv y \pmod 6$ admit perfect lethal sets.*

Proof. Consider the construction $(a, b, 2) + (8, 5, 5)$ for $a, b \in \{2, 5\} \pmod 6$, $a \not\equiv b \pmod 6$, and $a, b > 2$. Observe that this construction obtains all grids of the form described in (1) above, apart from $(10, 10, 7)$ and $(a, 7, 7)$, for $a \equiv 1 \pmod 6$.

By Corollary 3.2, we must show that the grids $(a, b, 2), (a, 5, 5), (8, b, 5), (8, 5, 2)$ are all perfect. By Proposition 3.6, $(a, b, 2)$ and $(8, 5, 2)$ are perfect. By Lemma 4.4, $(a, 5, 5)$ and $(8, b, 5)$ are perfect.

To obtain $(a, 7, 7)$, for $a \equiv 1 \pmod 6$, we consider $(4, 4, 4) + (a - 4, 3, 3)$. By Corollary 3.2, we must show that $(4, 4, 4), (4, 3, 3), (a-4, 4, 3), (a-4, 3, 4)$ are all perfect. By Constructions X and Y in Appendix A, we have that $(4, 4, 4)$ and $(4, 3, 3)$ are perfect, respectively. Since $a - 4 \equiv 3 \pmod 6$, we obtain $(a - 4, 4, 3)$ from Proposition 3.7.

To obtain $(10, 10, 7)$, consider $(5, 5, 5) + (5, 5, 2)$. By Corollary 3.2, we must show that $(5, 5, 5), (5, 5, 2), (5, 5, 2), (5, 5, 5)$ are all perfect. Lemma 4.4 gives us $(5, 5, 5)$, and Construction X gives us $(5, 5, 2)$. We conclude that all grids of the form given in (1) are perfect. □

Lemma 4.11. *All grids of the form* $(x, y, 7)$ *for* $x, y \in \{1, 4\}$ *and* $x \not\equiv y \pmod 6$ *are complete.*

Proof. Consider the construction $(a, b, 2) + (5, 5, 5)$ for $a, b \in \{2, 5\} \pmod 6$, $a \not\equiv b \pmod 6$, and $a, b > 2$. Observe that this construction obtains all grids of the form described in (2) above, apart from $(a, 7, 7)$, for $a \equiv 4 \pmod 6$.

By Corollary 3.2, we must show that the grids $(a, b, 2), (a, 5, 5), (5, b, 5), (5, 5, 2)$ are all perfect. By Proposition 3.6, $(a, b, 2)$ is perfect. We obtain $(a, 5, 5)$ and $(5, b, 5)$ from Lemma 4.4, and $(5, 5, 2)$ is given by Construction X.

To obtain $(a, 7, 7)$, for $a \equiv 4 \pmod 6$, we consider $(7, 4, 4) + (a - 7, 3, 3)$. Since $a \equiv 4 \pmod 6$ and $a \geq 7$, we have that $a \geq 10$. By Corollary 3.2, we must show that $(7, 4, 4), (7, 3, 3), (a - 7, 4, 3), (a - 7, 3, 4)$ are all perfect. We obtain $(7, 4, 4)$ from $(2, 2, 2) + (5, 2, 2)$. Constructions X and Y show that $(2, 2, 2), (2, 2, 2), (5, 2, 2), (5, 2, 2)$ are all perfect. Proposition 3.3 gives us $(7, 3, 3)$. Since $a - 7 \equiv 3 \pmod 6$, we obtain $(a - 7, 4, 3)$ from Proposition 3.7. We conclude that all grids of the form given in (2) are perfect. □

Lemma 4.12. *All grids of the form* $(x, y, 7)$ *for* $x, y \in \{0, 3\}$ *and* $x \equiv y \pmod 6$ *are complete.*

Proof. Consider the construction $(a, b, 2) + (6, 9, 5)$ for $a, b \in \{0, 3\} \pmod 6$, $a \not\equiv b \pmod 6$, and $a, b > 2$. Observe that this construction contains all grids described in (3) above, apart from $(9, 9, 7)$.

By Corollary 3.2, we must show that the grids $(a, b, 2), (a, 9, 5), (6, b, 5), (6, 9, 2)$ are all perfect. By Proposition 3.6, $(a, b, 2)$ and $(6, 9, 2)$ are perfect. By Proposition 3.5, $(a, 9, 5)$ is perfect. We obtain $(6, b, 5)$ from Lemma 4.4, for $b \geq 5$, and $(6, 3, 5)$ from Proposition 3.4.

To obtain $(9, 9, 7)$, consider $(6, 6, 4) + (3, 3, 3)$. By Corollary 3.2, we must show that $(6, 6, 4), (6, 3, 3), (3, 6, 3), (3, 3, 4)$ are all perfect. We obtain $(6, 6, 4)$ from $(3, 3, 1) + (3, 3, 3)$. Constructions X and Y show that $(3, 3, 1), (3, 3, 3), (3, 3, 3), (1, 3, 3)$ are all perfect. Proposition 3.3 gives us $(6, 3, 3)$ and $(4, 3, 3)$. We conclude that all grids of the form given in (3) are perfect. □

Lemma 4.13. *All grids of the form* $(x, y, 7)$ *for* $x, y \in \{0, 3\}$ *and* $x \not\equiv y \pmod 6$ *are complete.*

Proof. Consider the construction $(a, b, 2) + (6, 6, 5)$ for $a, b \in \{0, 3\} \pmod 6$, $a \not\equiv b \pmod 6$, and $a, b > 2$. Observe that this construction contains all grids described in (4) above.

By Corollary 3.2, we must show that the grids $(a, b, 2), (a, 6, 5), (6, b, 5), (6, 6, 2)$ are all perfect. By Proposition 3.6, $(a, b, 2)$ is perfect. We obtain $(6, b, 5)$ from Lemma 4.4, for $b \geq 5$, and $(6, 3, 5)$ from Proposition 3.4. We obtain $(6, 6, 2)$ by Construction X. We conclude that all grids of the form given in (4) are perfect. □

Lemma 4.14. *Thickness 7 is complete.*

Proof. By Lemmas 4.10, 4.11, 4.12, and 4.13, all divisibility cases for thickness 7 admit perfect lethal sets. □

4.5 Completeness of Grids of Size ≥ 5

We can get completeness in every residue class modulo 3 by simply considering the grids obtained from $(x, y, z) + (3, 3, 3)$.

Chapter 5
Tight Bound on (a, b, c) Grids for $a \geq b \geq c \geq 11$

Chapter 6
Thickness One

While results from the previous chapters resolve the question of $m(a_1, a_2, a_3, 3)$ for $a_1 \geq a_2 \geq a_3 \geq 11$, similar constructions for smaller grids remain sparse. Nevertheless, computer examples seem to suggest that grids of minimum size at least 2 are largely optimal. Grids of thickness 1 tell a different story. In this chapter, we prove that the only perfect grids in thickness 1 are those of the form $[2^n - 1]^2$. This answers a question posed by Benevides et al. in [**?**].

6.1 A tight result for $[n]^2$

The argumentative structure of the proof is as follows: Let A_0 be a perfect lethal set on the grid $(a_1, a_2, 1)$. We show that the structure of A_0 guarantees the existence of a perfect lethal set on the smaller grid $(\frac{a_1-1}{2}, \frac{a_2-1}{2}, 1)$. Repeated applications of this process of reduction guarantee the existence of a perfect lethal set on the grid $(a_0, 1, 1)$. Since the only such grid that admits a perfect lethal set is $(1, 1, 1)$, we are forced to conclude that $a_1 = a_2 = 2^k - 1$ for some $k > 0$.

6.1.1 Preliminaries

For the remainder of the chapter, let $G = [a_1] \times [a_2]$. Recall that perfect lethal sets match the surface area bound. In particular,

$$|A_0| = \frac{a_1 a_2 + a_1 + a_2}{3}.$$

We begin with the following observations regarding the structure of A_0:

Proposition 6.1. *If A_0 is a perfect lethal set on G, then A_0 contains alternating vertices along the border of G.*

Proof. Since A_0 is perfect, it must form an independent set in G. By Proposition 2.6, no two adjacent border vertices are both uninfected. Together, these conditions ensure that A_0 intersects the border of G in an alternating pattern (see Figure 6.2). □

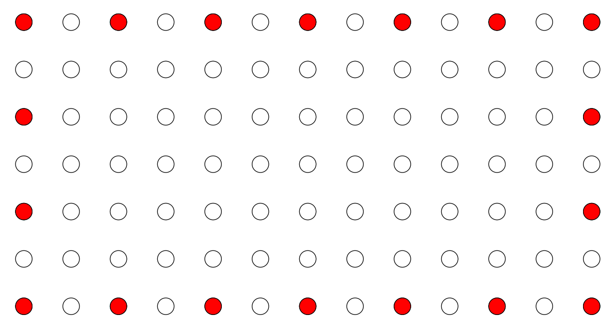

Figure 6.1: Alternating infection along the border of $[7] \times [13]$.

Proposition 6.2. *If A_0 is a perfect lethal set on G, then $a_1, a_2 \equiv 1 \pmod 2$.*

Proof. By Propositions 6.1 and 2.5, $a_1, a_2 \equiv 1 \pmod 2$. □

Proposition 6.3. *Let A_0 be a perfect lethal set on $[a_1] \times [a_2]$ under 3-neighbor percolation. Let $H = V([a_1] \times [a_2]) \setminus A_0$. Then the subgraph induced by H is acyclic and each component of H contains exactly one border vertex.*

Proof. Sufficiency follows from Proposition 2.7. For necessity, observe that the interior vertices of A_0 each remove exactly 4 edges from the subgraph induced by H. This implies that the subgraph induced by H is a forest with exactly $a_1 + a_2 - 2$ components. As there are exactly $a_1 + a_2 - 2$ border vertices in H, each component must contain exactly one border vertex. □

Consider a labeling of the vertices of G by their coordinates, starting at $(1, 1)$ in the lower left and ranging to (a_1, a_2) in the upper right. Refer to a vertex (x, y) as "even" or "odd" depending on the parity of $x + y$. If a set $S \subseteq V(G)$ contains all vertices of the same parity, call S monochromatic. The following lemma leverages the prior propositions to prove that any perfect lethal set on G must be monochromatic.

Lemma 6.4. *Let A_0 be a perfect lethal set on G. Then A_0 is monochromatic with respect to the proper 2-coloring of G.*

Proof. From Proposition 6.1, observe that A_0 contains all even vertices along the border of G. Suppose for contradiction that A_0 also contains odd vertices. We show that this implies the existence of a cycle in the subgraph induced by $V(G) \setminus A_0$, contradicting Proposition 6.3.

Let H be a graph with vertices $V(H) = V(G)$ and edges uv if and only if u and v are diagonally adjacent in G. Consider the subgraph of H induced by the odd vertices of A_0 and let K be a connected component. Observe that K is acyclic: any cycle in K encloses a component of $G[\overline{A_0}]$, contradicting Proposition 6.3. Furthermore, by Proposition 6.1, all vertices of K are in the interior of G. Let C_H be the cycle induced in H by $N_G(K)$. Note that since A_0 is an independent set, $N_G(K) \cap A_0 = \emptyset$ and $C_H \cap A_0 = \emptyset$. Consider

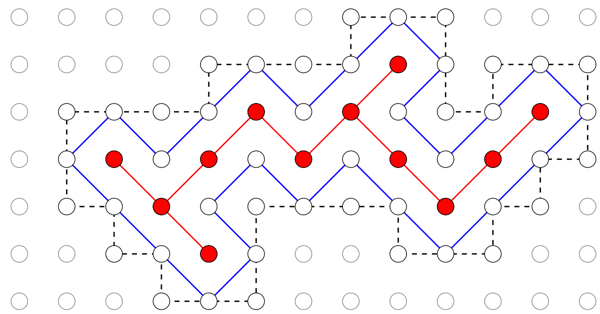

Figure 6.2: $[7] \times [13]$ grid with component K (red), C_H (blue), and C_G (dashed).

the closed walk induced in G by the vertices $V(C_H) \cup N_H(K) \setminus A_0$. This walk describes a cycle C_G in $G[\overline{A_0}]$, which contradicts Proposition 6.3. $\square$

6.1.2 Reduction

We present an auxiliary $(\frac{a_1-1}{2}, \frac{a_2-1}{2}, 1)$ grid G' obtained from G, and show that it admits a perfect lethal set. Let the vertices of G' be 2×2 tiles of G given by

$$\{(2x-1, 2y-1), (2x-1, 2y), (2x, 2y-1), (2x, 2y) \mid (x, y) \in [1, (a_1-1)/2] \times [1, (a_2-1)/2]\},$$

with adjacencies between tiles that differ by one in each of the cardinal directions. Note that Proposition 6.2 ensures that $|V(G')|$ is an integer. Furthermore, observe that for any tile $T_{x,y} \in V(G')$, $|A_0 \cap T_{x,y}| \in \{1, 2\}$. This follows from the fact that A_0 is an independent set, and $G[\overline{A_0}]$ is acyclic. For all $T_{x,y} \in V(G')$, color $T_{x,y}$ blue if $|A_0 \cap T_{x,y}| = 2$, and white otherwise. Let b and w be the number of blue and white tiles in $V(G')$, respectively. We determine b by solving the following system of equations:

$$\begin{aligned} b + w &= \frac{(a_1-1)(a_2-1)}{4} \\ 2b + w &= \frac{a_1 a_2 + a_1 + a_2}{3} - \frac{a_1 + a_2}{2}. \end{aligned}$$

This gives the following expression for b:

$$\begin{aligned} \frac{a_1 a_2 + a_1 + a_2}{3} - \frac{a_1 + a_2}{2} - \frac{(a_1-1)(a_2-1)}{4} &= \frac{a_1 a_2 + a_1 + a_2 - 3}{12} && (6.1) \\ &= \frac{(\frac{a_1-1}{2})(\frac{a_2-1}{2}) + \frac{a_1-1}{2} + \frac{a_2-1}{2}}{3}. && (6.2) \end{aligned}$$

Note that this is precisely the surface area bound for the $(\frac{a_1-1}{2}, \frac{a_2-1}{2}, 1)$ grid. Furthermore, since $a_1 \equiv a_2 \equiv 1 \pmod 6$ or $a_1 \equiv a_2 \equiv 3 \pmod 6$, all terms on the LHS of 6.1 are integral, and so the SA bound in 6.2 is tight.

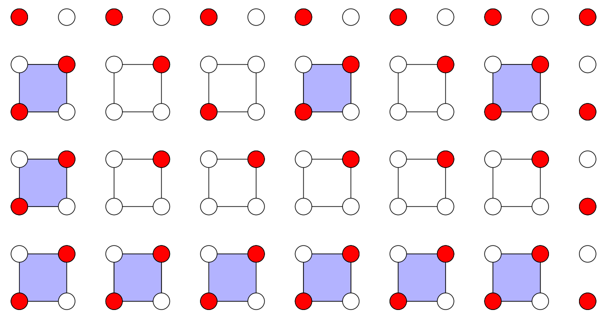

Figure 6.3: $[7] \times [13]$ grid with $T_{x,y}$ colored blue if $|T_{x,y} \cap A_0| = 2$. Note that A_0 is *not* perfect.

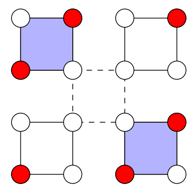

Figure 6.4: Diagonal white tiles and the resulting 4-cycle.

We prove that the blue tiles form a lethal set in G'. We begin with the following observation:

Proposition 6.5. *All white tiles have their A_0-vertex in the bottom left corner.*

Proof. For contradiction, suppose that there exists a white tile T_0 with one infected vertex in the upper right. By Proposition 6.3, there exists a path in $G[\overline{A_0}]$ from $T_0 \setminus A_0$ to the border. We consider the sequence of white tiles $T_0, \ldots, T_n$ containing this path.

Consider two consecutive tiles T_i, T_{i+1} in this sequence. Note that T_i and T_{i+1} cannot be diagonally adjacent, as such a configuration creates a 4-cycle in $G[\overline{A_0}]$ (see Figure 6.4). Additionally, by Proposition 6.1, observe that T_n has its infected vertex in the bottom left corner. Therefore, since T_0 contains an infection in the top right by assumption, there exist tiles T_i, T_{i+1} such that T_i has an infection in the top right, and T_{i+1} has an infection in the bottom left.

We consider two cases. If T_{i+1} is below or to the left of T_i, we obtain a 4-cycle. On the other hand, if T_{i+1} is above or to the right of T_i, there is no path in $G[\overline{A_0}]$ between them (see Figure 6.5). We therefore conclude that T_0 must have an infected vertex in the bottom left. $\square$

We are now prepared to prove that the blue tiles form a lethal set in G'.

Lemma 6.6. *The set of blue tiles is lethal and perfect in $[(a_1 - 1)/2] \times [(a_2 - 1)/2]$ under 3-neighbor percolation.*

Proof. In Equation 6.2, we saw that the number of blue tiles matches the lower bound for 3-neighbor percolation in $[(a_1 - 1)/2] \times [(a_2 - 1)/2]$. We now show that the 3-

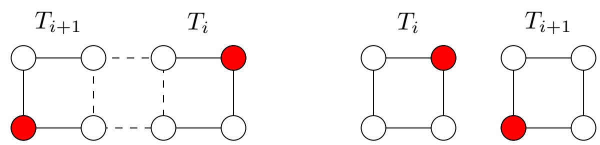

Figure 6.5: Possible configurations of adjacent white tiles.

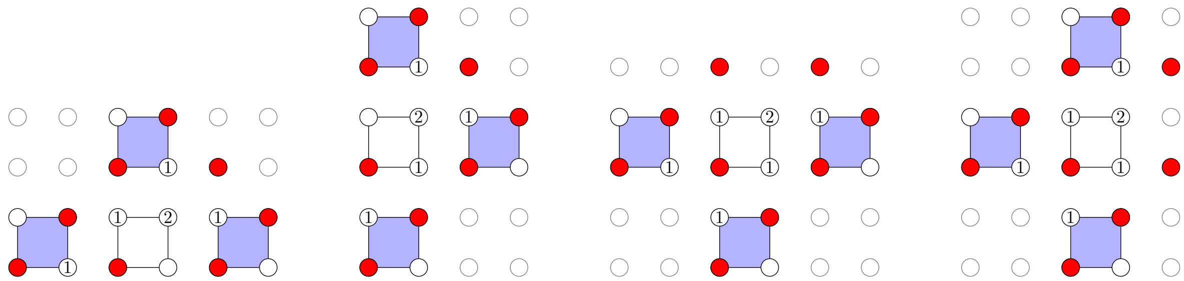

Figure 6.6: The four configurations of blue tiles leading to infection.

neighbor process infects white tiles if and only if they are adjacent to at least 3 blue tiles.

For sufficiency, consider the four cases illustrated in Figure 6.6. In each of these configurations, the upper right vertex of the white tile (labeled with a "2") becomes infected after two iterations. Each case requires the assistance of one to two extra infections outside of the three blue tiles. However, these infections constitute the bottom left vertex in adjoining tiles, which is always infected.

For necessity, we show that any cycle or border-to-border path in the white tiles of G' implies a cycle or border-to-border path in $G[\overline{A_0}]$. Observe that, by Proposition 6.5, the vertices $(T_i \cup T_j) \setminus A_0$ of any adjacent white tiles T_i, T_j induce a connected component in G. Therefore, any cycle or border-to-border path in G' implies the existence of a cycle or border-to-border path in $G[\overline{A_0}]$. We conclude that the blue tiles form a perfect lethal set in $[(a_1-1)/2] \times [(a_2-1)/2]$ under 3-neighbor percolation. $\square$

6.1.3 Conclusion

In the prior sections, we have shown that the existence of a perfect lethal set on $[a_1]\times[a_2]$ implies the existence of a perfect lethal set on $[(a_1-1)/2] \times [(a_2-1)/2)]$. Proposition 6.2 mandates that all perfect lethal sets on $[a_1] \times [a_2]$ be odd-by-odd. Together, these statements require that $a_1 = 2^{k_1} - 1$ and $a_2 = 2^{k_2} - 1$ for some $k_1, k_2 > 0$, respectively. By repeated applications of Lemma 6.6, we ultimately obtain a grid $[a_0] \times [1]$ that admits a perfect lethal set. Clearly, the only such grid is the single vertex [1]. We therefore conclude that the only two-dimensional grids that admit perfect lethal sets under 3-neighbor percolation are square grids of the form $[2^n - 1]^2$. The construction that achieves this is published in Benevides et al [**?**], and reproduced as Construction

7.1 in Chapter 7.

Chapter 7
Constructions

7.1 Introduction

In this chapter, we present diagrammed proofs of lethal sets that percolate at the lower bound. The proofs are organized by the thickness of the grid. Many of the constructions in the following sections belong to infinite families of either optimal or perfect sets. In this case, we shall examine the grids by region, and observe that certain regions can be expanded to arbitrarily large sizes using mathematical induction.

We shall call a thickness *semi-complete* if all divisibility cases are optimal.

7.2 Thickness 1

There are two general constructions in thickness 1 that percolate at the surface area bound. The first construction is perfect for all $(2^n-1, 2^n-1, 1)$ grids, and originates in a 2021 paper by Benevides et al. [**?**]. The second construction is optimal for all grids $(a, b, 1)$, where $a \equiv 5 \pmod 6$, $b \equiv 1 \pmod 2$, and $a, b \geq 5$. As such grids constitute non-divisibility cases, this construction is not perfect.

7.2.1 Purina

We refer to this construction colloquially as the Purina construction, due to the similarly between its instance on the $(3, 3, 1)$ grid and the logo of the pet food brand. No funding has been offered, but we are open to the possibility. A more extensive discussion on this pattern can be found in [**?**].

Construction 7.1. *All grids of the form* $(2^n-1, 2^n-1, 1)$ *are perfect.*

Proof. This is a recursive construction built from the base component piece shown in figure 7.1. Note that this $(3, 3, 1)$ construction is lethal under the 3-neighbor bootstrap

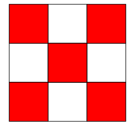

Figure 7.1: A perfect percolating set for $(3,3,1)$.

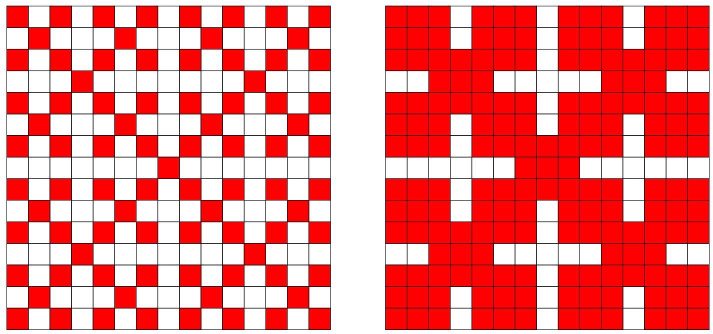

Figure 7.2: A perfect percolating set for $(15,15,1)$.

process, and that it meets the surface area bound:

$$\frac{1}{3}\cdot(ab+bc+ca)=\frac{1}{3}\cdot(9+3+3)=5.$$

For larger grids of size $(2^n-1,2^n-1,1)$, join four copies of $(2^{n-1}-1,2^{n-1},1)$ about two perpendicular corridors, and infect the vertex at their intersection (figure 7.2). Observe that the resulting set is lethal: each of the four smaller grids is lethal by hypothesis, and the remaining vertices induce a forest with disconnected boundary points, which percolates by lemma **??**. Furthermore, note that

$$\begin{aligned}\text{S.A.}(2^n-1,2^n-1,1)&=\frac{1}{3}\cdot(2^{2n}-1)\\&=4\cdot\frac{1}{3}\cdot(2^{2n-2}-1)+1=4\cdot\text{S.A.}(2^{n-1}-1,2^{n-1},1)+1,\end{aligned}$$

and therefore this construction is perfect. □

7.2.2 Snakes

As indicated by lemma **??**, a fundamental characteristic of lethal sets S is the presence of an initially uninfected corridor, bounded by walls of infection. This structure is apparent in the second diagrams of figures 7.2 and 7.5. These corridors correspond to forests in the complement $G[\overline{S}]$ of S. In this subsection, we provide a general method for constructing such corridors in $(a,b,1)$ grids where $a\equiv 5 \pmod 6$ and $b\equiv 1 \pmod 2$.

Construction 7.2. *All grids of the form* $(a,b,1)$, $a\equiv 5 \pmod 6$, $b\equiv 1 \pmod 2$, *and* $a,b\geq 5$ *are optimal.*

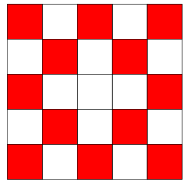

Figure 7.3: An optimal percolating set for $(5, 5, 1)$.

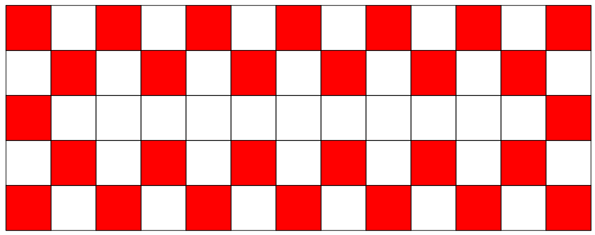

Figure 7.4: An optimal percolating set for $(5, 13, 1)$.

Proof. For grids of the form $(a, b, 1)$, $a \equiv 5 \pmod 6$, $b \equiv 1 \pmod 2$, we construct an optimal infected set and show that it percolates by lemma **??**. For the base case, consider the $(5, 5, 1)$ grid G illustrated in figure 7.3. Observe that this construction is optimal. Now consider the grid G' resulting from the insertion of a $(5, 2k, 1)$ block, as shown in figure 7.4. Note that the subgraph induced by the uninfected vertices of G' satisfies the conditions of lemma **??**. Furthermore, note that if any $(5, n, 1)$ grid is optimal, the $(5, n+2, 1)$ grid resulting from such a construction has surface area bound S.A.$(5, n, 1) + 4$, which agrees with the number of infected vertices.

To extend this construction in the vertical direction, we introduce a kink in the snaking infection. This kink requires six rows to produce a repeating pattern. The structure of this design is shown in figure 7.5. For grids of smaller width, the same construction gives optimal percolating sets; however, the snaking pattern is increasingly difficult to recognize in thin grids. $\square$

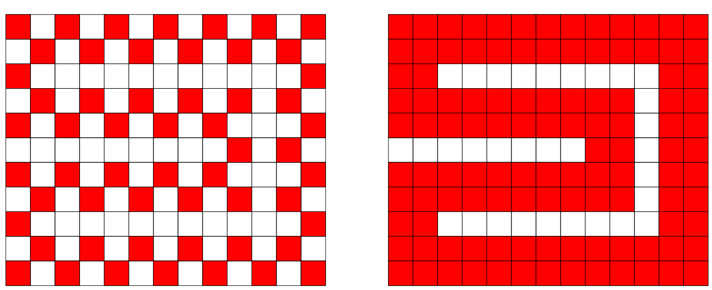

Figure 7.5: An optimal percolating set for $(11, 13, 1)$.

7.3 Thickness 2

In this section we examine four infinite families of perfect grids. We show that each has a manifold that admits a lethal set of perfect size. We note that such lethal sets are likely to exist for nearly all divisibility cases in thickness two; however, constructions are elusive and those presented here are sufficient to prove the main result of this thesis.

Unlike those presented in the previous section, the following proofs all leverage lemma 2.1. As a consequence, their argumentative structure remains broadly the same, even as the constructions themselves appear quite different. For this reason, we shall outline this structure here, before examining the specific proofs.

We begin by demonstrating that a grid G admits a manifold M. To show so, we identify the regions $R_1, \ldots, R_k$ that partition $V(G) \setminus M$. In our diagrams, these regions are represented by the volumes enclosed by three perpendicular blue, green, and red walls. We then identify a proper unfolding H of M and show that H admits a lethal set A, where $|A| = \mathrm{SA}(G)$. Finally, we apply corollary **??** to prove that G is perfect.

Construction 7.3. *All* $(a, 3, 2)$ *grids with* $a \equiv 0 \pmod 6$ *are perfect.*

Proof. Let G be an $(a, 3, 2)$ grid with $a \equiv 0 \pmod 6$, and let M be a manifold of G and H be its proper unfolding (see figure 7.7). Observe that M is indeed a manifold: it partitions $V(G) \setminus M$ into two sets R_1 and R_2, both bounded by mutually orthogonal red, green, and blue faces (see figure 7.7). Furthermore, note that H is obtained from M by cutting along seams between red and green faces, and flattening the figure. It follows that H is a proper unfolding of G. We show that H admits a perfect lethal set.

Consider the initial infection A of H illustrated in figure 7.8. Observe that A infects all vertices of H by lemma **??**, with the exception of two regions on the far left and far right. However, note that upon refolding, the two cells marked with an "X" in H represent the same cell in G. This is sufficient to infect the remaining regions of H, and by corollary **??**, A is lethal on G. Finally, a simple calculation reveals that $|A|$ matches the surface area bound, and therefore is perfect.

We can extend this construction in the x direction by inserting the repeated structure of six columns; this augmentation percolates by lemma **??** and agrees with the surface area bound for all larger grids. This completes the proof. □

Construction 7.4. *All* $(a, 3, 2)$ *grids with* $a \equiv 3 \pmod 6$ *are perfect.*

Proof. (This construction is the same as the previous one, except the the final four columns are augmented slightly to accommodate the $0 \pmod 3$ requirement. Instead of deriving a proper unfolding, it is probably easier to simply show that this small change is sufficient to guarantee lethality, and agrees with the S.A. bound.) □

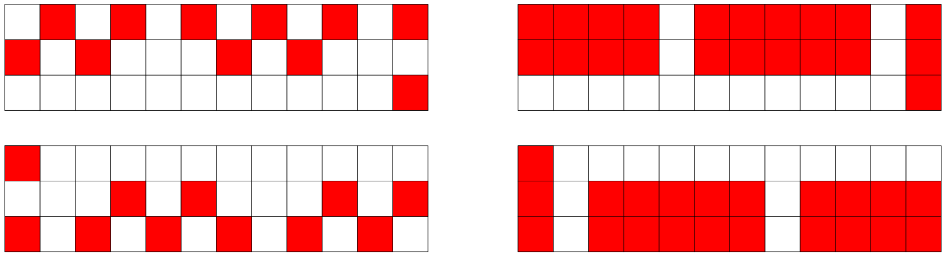

Figure 7.6: A perfect percolating set for $(3, 12, 2)$.

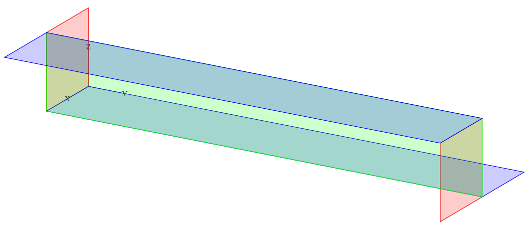

(a) A manifold of $G = (3, 12, 2)$.

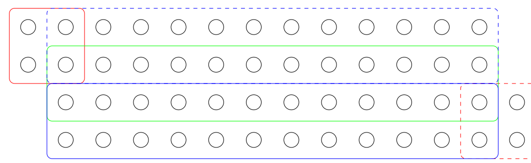

(b) A proper unfolding of G.

Figure 7.7: A proper unfolding of $G = (3, 12, 2)$. Colored rectangles indicate faces of G. Dashed lines indicate that cells appear on different layers.

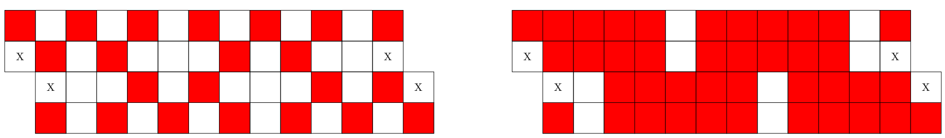

Figure 7.8: A percolating set on the proper unfolding of $G = (3, 12, 2)$.

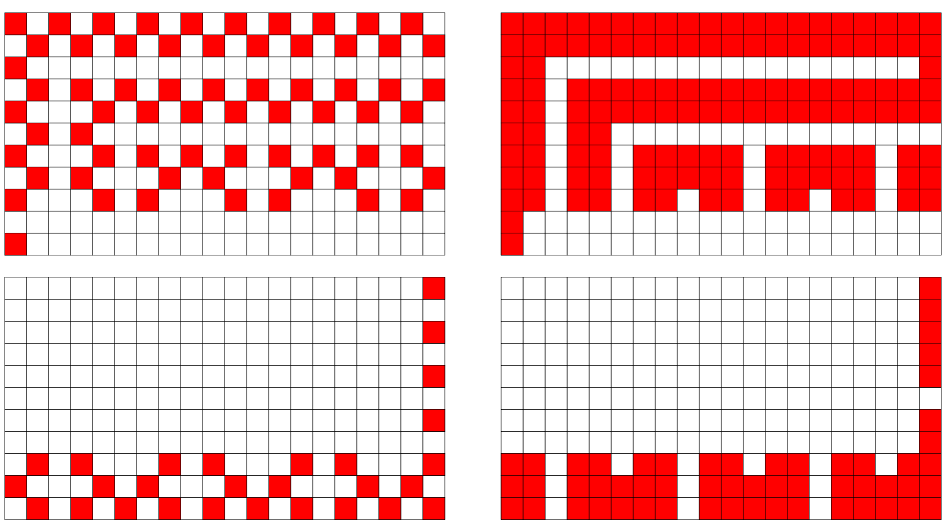

Figure 7.9: A perfect percolating set for $(11, 20, 2)$.

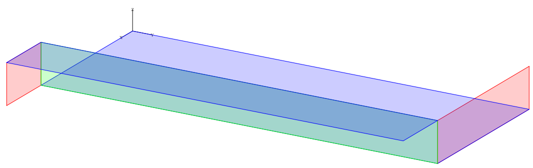

(a) A manifold of $G = (11, 20, 2)$.

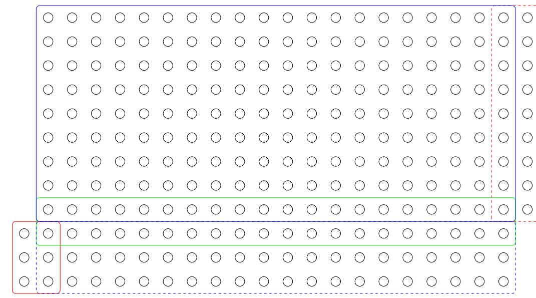

(b) A proper unfolding of G.

Figure 7.10: A proper unfolding of $G = (11, 20, 2)$. Colored rectangles indicate faces of G. Dashed lines indicate that cells appear on different layers.

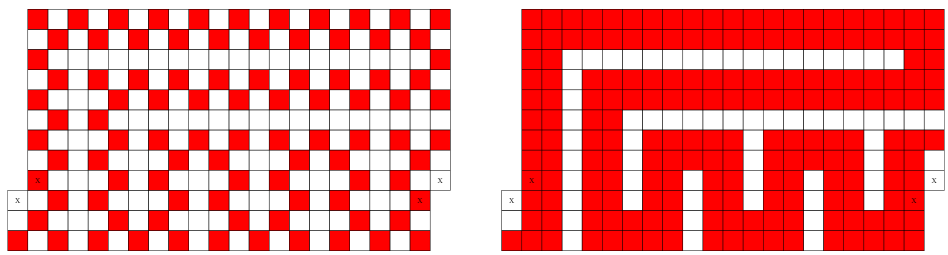

Figure 7.11: A percolating set on the proper unfolding of $G = (11, 20, 2)$.

Construction 7.5. *All $(a, b, 2)$ grids with $a, b \in \{2, 5\} \pmod 6$, $a \neq b \pmod 6$, and $a, b > 2$ are perfect.*

Proof. Let G be an $(a, b, 2)$ grid with $a, b \in \{2, 5\} \pmod 6$ and $a \neq b \pmod 6$, and let M be a manifold of G and H be its proper unfolding (figure 7.10). Note that M partitions the vertices of $V(G) \setminus M$ into two disjoint sets R_1 and R_2, both bounded by mutually orthogonal red, green, and blue faces. Note, also, that H is obtained from M by cutting along seams between red and green faces, and flattening the figure. Therefore, H is a proper unfolding of G. We show that H admits a perfect lethal set.

Consider the initial infection A of H as shown in figure 7.11. By lemma **??**, A infects all vertices of H, with the exception of two regions on the left- and right-most sides of the grid. However, note that the vertices labeled "X" in figure 7.11 represent that same vertex in G. This permits A to infect the remaining healthy vertices, thereby proving that A is lethal on H. By corollary **??**, A is lethal on G. Finally, a simple calculation shows that $|A|$ satisfies the surface area bound on G, and so A is perfect.

The above construction holds for $a \geq 5$ and $b \geq 8$. It can be extended in the x direction by inserting a block of width 6, representing the repeating vertical snaking pattern. Similarly, it can be extended in the y direction by inserting a block of height 6, representing the horizontal snaking pattern. Both such augmentations spawn infections that satisfy the conditions of lemma **??**, and a simple calculation reveals that they agree with the surface area bound. This concludes the proof. $\square$

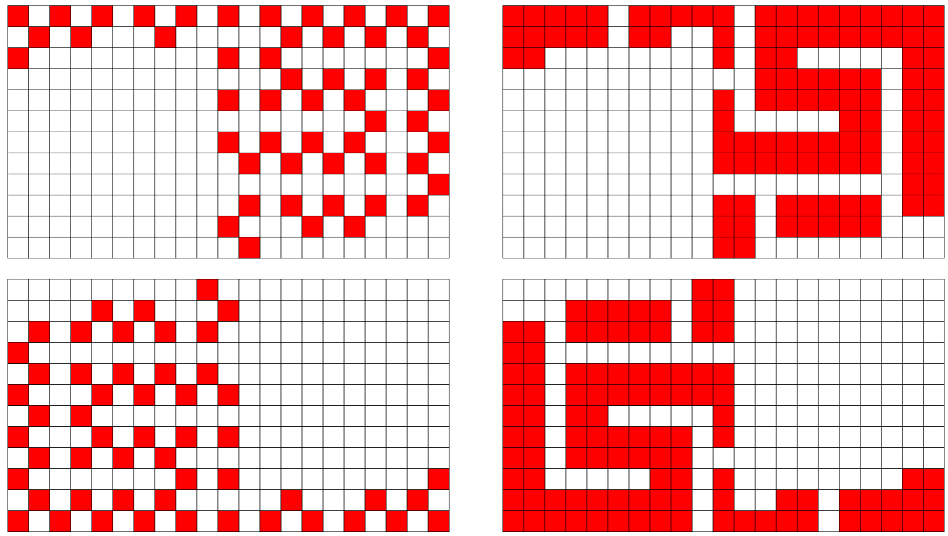

Figure 7.12: A perfect percolating set for $(12, 21, 2)$.

Construction 7.6. *All* $(a, b, 2)$ *grids with* $a, b \in \{0, 3\} \pmod 6$ *and* $a \neq b \pmod 6$ *are perfect.*

Proof. Consider the $(21, 12, 2)$ grid G shown in figure 7.12. Let H be a unfolding of G (figure 7.13). Observe that H is proper: three mutually orthogonal faces of G_1 are shown by blue, green and dashed red regions, and mutually orthogonal faces of G_2 are shown by the red, green and dashed blue regions. We show that H admits a lethal set of size S.A.$(12, 21, 2) = 106$. Consider such a set, as shown in figure 7.14. (Observe that this is the same set as shown in figure 7.12.) By lemma **??**, this set percolates with the exception of two C_4s in the top and bottom of the grid. However, notice that one of these cells is a duplicate of an already infected cell. (This duplication is a consequence of the proper unfolding of G.) Therefore, H admits a lethal set, and by corollary **??**, G is perfect.

For all larger grids, observe that the snaking corridor in the left side G can be extended by multiples of 6 in both the x and y directions. These resulting grid still percolates under lemma **??**. A simple calculation verifies that such an alteration produces initial infections at the surface area bound. □

7.4 Thickness 3

Construction 7.7. *All* $(a, b, 3)$ *grids* G *with* $a \equiv 3 \pmod 6$ *and* $b \equiv 1 \pmod 2$ *are perfect.*

Proof. Consider the grid $H = (a + 2, b + 2, 1)$, and observe that such a grid admits an

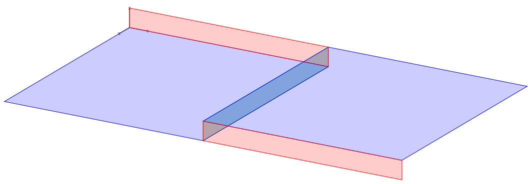

(a) A manifold of $G = (12, 21, 2)$.

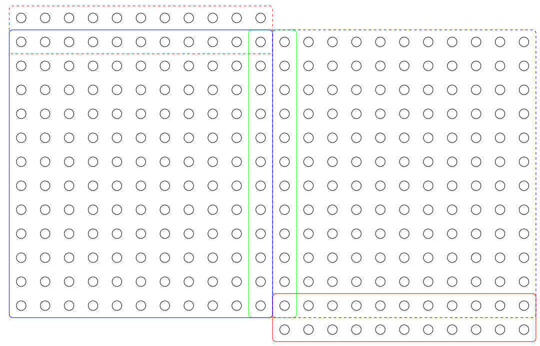

(b) A proper unfolding of G.

Figure 7.13: A proper unfolding of $G = (12, 21, 2)$. Colored rectangles indicate faces of G. Dashed lines indicate that cells appear on different layers.

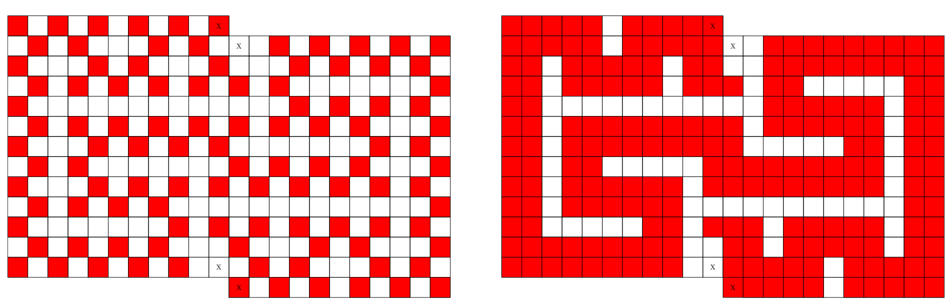

Figure 7.14: A percolating set on the proper unfolding of $G = (12, 21, 2)$.

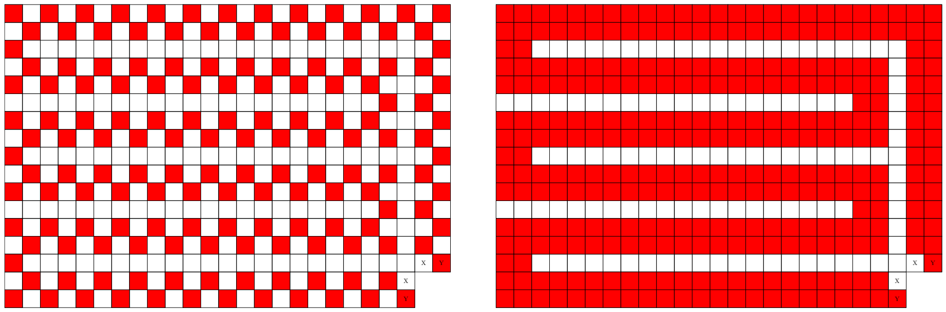

Figure 7.15: A percolating set on the proper unfolding H' of $G = (15, 23, 3)$.

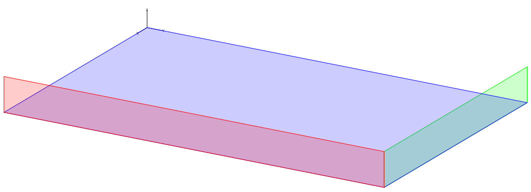

(a) A manifold of $G = (15, 23, 3)$.

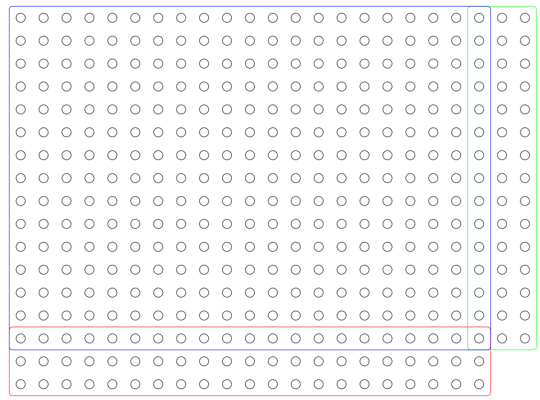

(b) A proper unfolding of G.

Figure 7.16: A proper unfolding of $G = (15, 23, 3)$. Colored rectangles indicate faces of G.

optimal percolating set by construction 7.2. Note that

$$\mathrm{SA}(a, b, 3) = \lceil \mathrm{SA}(a + 2, b + 2, 1) \rceil - 3.$$

We show that an unfolding of G can be obtained from a simple augmentation of H. Let H' be the grid obtained by deleting the four vertices in the bottom, right-most corner of H (see figure 7.15). Consider the folding pattern illustrated in figure 7.16, and observe that the pairs of vertices adjacent to the deleted region are duplicates of each other. (In other words, consider folding up the red and green regions in figure 7.16, and notice that this operation causes vertices to overlap.) Taking this into account, the unfolding of G percolates by lemma **??**. Since H admits an optimal percolating set of size $\lceil \mathrm{SA}(a+2, b+2, 1) \rceil$, and precisely 3 of the vertices deleted from H to obtain H' were infected, it follows that the unfolding of G percolates at the lower bound. Finally, by lemma **??**, since the unfolding of G is proper and percolates at the lower bound, G is perfect. $\square$

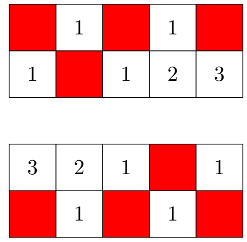

Figure 7.17

7.5 Individual constructions

In this section, we diagram lethal set constructions for single grids. The initial infection A is colored red, and all other cells are labeled with the time t that they are first infected.

Construction 7.8. *The grid* $(5, 2, 2)$ *is perfect.*

Proof. See figure 7.17. □

Construction 7.9. *The grid* $(5, 5, 5)$ *is perfect.*

Proof. See figure 7.18. □

Construction 7.10. *The grid* $(8, 5, 5)$ *is perfect.*

Proof. See figure 7.19. □

20	19	18	17	
9	8	7		1
	1		1	
11	8	1	6	7
12	9		7	8

19	18	17	16	15
	1	6	7	8
1		1	4	5
10	7		5	6
11	8	1	6	7

18	17		13	14
9		5	8	9
8	5	4	3	
9	6	3	2	1
10	7		1	

17	16	11	12	13
12	11	10	9	10
7	6	5		1
	5	4	1	
1		1		1

	15		1	
13	14	11		11
	15	16	17	18
1	16	17	18	19
	17	18	19	20

Figure 7.18

	1		33	34	35	36	37
37	30	23	22	21	20	19	
38	31	10	9		9	16	17
39	32	9	8	7	8	15	18
40	33		1		1		19

1		25	32	33	34	35	
36	29	24	21	20	19	18	17
37	30	9	8	7		15	16
38	31	8	7	6	5	14	15
39	32	7		1		1	

	29	30	31	32	33	36	37
35	28	25		13	14	15	18
36	9		1	8	9	14	15
37	8	5		3	4	13	
	7	6	1	2	3	14	15

33	32	31		13		37	38
34	27	26	1	12	11		19
35		3	2	9	10	11	
38	5	4	1		1	12	1
39		1		1		15	16

	33	34	35	36	37	38	39
1		27		33	34	35	36
	1	28	29	32	33	34	35
39	30	29	30	31		13	
40	31		31	32	33	34	35

Figure 7.19

Chapter 8
Programmatic Approach

Chapter 9
Torus

9.1 Introduction

I know I shouldn't be working on this now but I have some ideas. We can use Benevides proof of the lower bound for the torus, which states the following:

Lemma 9.1. *Let $T = C_n \,\square\, C_m$ be the $n \times n$ torus. Let A be a lethal set on T. Then $|A| \geq \frac{nm+c}{3}$, where c is the number of components in the graph $T[\overline{A}]$.*

There are some nice observations to be made here. First, in much the same way that loss of surface area contributes to fractional increases in the surface area bound for grid graphs, the number of components can be understood to indicate sub-optimality in the torus. As a particular example, the torus $T = C_18 \,\square\, C_12$ has lower bound of 72.33. This can be obtained from an optimal (but not perfect) thickness one grid construction for $(17, 11, 1)$, with an additional vertex in the bottom rightmost corner.

There's something interesting happening here. In this particular case, $T[\overline{A}]$ has three components. Assuming the best case scenario (where it has one component), we get the lower bound of 72.33. However, if we instead consider three components, the lower bound sits precisely as 73. As the construction of T simple involves adding an additional vertex to an optimal (not perfect) grid construction, it appears as though the inadequacies of the grid construction (namely, cells that are infected by 4 neighbors) somehow translate directly to inadequacies of the torus construction (multiple components in the complement).

Oh wait, is this just because the surface area argument is fundamentally an argument about the number of components in the complement? I think it is. Every time you lose surface area, you've deleted a tree from the forest (because in order to remove the final vertex in a tree, you need an inefficiency–unless the tree sits on the boundary). Therefore, it makes sense that the best solutions on the torus have exactly one component in the complement.

How does the surface area argument map to an argument about components? Knowing this should allow us to construct a lower bound on the 4D torus.

There are other questions regarding some form of algebraic or numerical equivalence between expressions for the lower bounds of tori and grids. It is clear that

Chapter 10
Conclusion

Bibliography

[1] J. Balogh and B. Bollobás. Bootstrap percolation on the hypercube. *Probability Theory and Related Fields*, 134(4):624–648, 2006.

[2] J. Chalupa, P. L. Leath, and G. R. Reich. Bootstrap percolation on a bethe lattice. *Journal of Physics C: Solid State Physics*, 12(1):L31, 1979.